Infectious Disease Modelling 9 (2024) 329–353

Contents lists available at ScienceDirect

Infectious Disease Modelling

journal homepage: www.keaipublishing.com/idm

Mathematical modeling of contact tracing and stability analysis to inform its impact on disease outbreaks; an application to COVID-19

Mohamed Ladib [a], Aziz Ouhinou [a, *], Abdul-Aziz Yakubu [b]

[a] University of Sultan Moulay Slimane, Faculty of Sciences and Techniques, Team of Mathematics and Interactions, Béni-Mellal, Morocco
[b] Howard University, Dept Math, Washington, DC, 20059, USA

ARTICLE INFO

Article history:
Received 29 October 2023
Received in revised form 29 January 2024
Accepted 29 January 2024
Available online 2 February 2024
Handling Editor: Dr Daihai He

JEL classification:
39A20
39A30
92B05

Keywords:
Mathematical modeling
Infectious diseases
Discrete systems
Disease-age structured populations
Contact tracing
Effective reproduction number
COVID-19

ABSTRACT

We develop a mathematical model to investigate the effect of contact tracing on containing epidemic outbreaks and slowing down the spread of transmissible diseases. We propose a discrete-time epidemic model structured by disease-age which includes general features of contact tracing. The model is fitted to data reported for the early spread of COVID-19 in South Korea, Brazil, and Venezuela. The calibrated values for the contact tracing parameters reflect the order pattern observed in its performance intensity within the three countries. Using the fitted values, we estimate the effective reproduction number $\mathcal{R}_e$ and investigate its responses to varied control scenarios of contact tracing. Alongside the positivity of solutions, and a stability analysis of the disease-free equilibrium are provided.

1. Introduction

Throughout history, almost all emerging diseases have posed a serious danger and caused a state of extreme alert. The recently emerged pandemic COVID-19 presented a great challenge for the whole world, causing over 6.9 million deaths by late November 2023 (Dashboard of covidb). It began spreading first in China and slowly made its way to the other countries of the globe. Due to the easy transmission of the pathogen between individuals, most governments swiftly responded with standard non-pharmaceutical interventions (NPIs) such as the full lockdown of cities, the shut-down of airports, strict social distancing, and the testing of suspected individuals with history travels from corrupted places (Perra, 2021; Schneiders et al., 2022). The contact tracing intervention also gained attention during that period. Especially, when no vaccines were yet available. It was a

* Corresponding author.
E-mail addresses: mohamedladib1995@gmail.com (M. Ladib), a.ouhinou@usms.ma (A. Ouhinou).
Peer review under responsibility of KeAi Communications Co., Ltd.

https://doi.org/10.1016/j.idm.2024.01.010

useful control strategy to help contain outbreaks faster with minimum casualties (Hossain et al., 2022). In fact, the careful screening of confirmed cases and the isolation of their contactees can cause an early interception of further infections, which slows down the spread of epidemics.

From a mathematical perspective, modelling the process of contact tracing itself, was also subject of study for numerous research papers (Browne, Gulbudak, & Webb, 2015; Huo, 2015; Hyman, Li, & Stanley, 2003; Kwok et al., 2019; Müller & Kretzschmar, 2021a; Rusu, Emonet, & Farrahi, 2021; Tsimring & Huerta, 2003). Different approaches to address the question were followed. For example, in (Browne et al., 2015), authors considered a deterministic model for EBOLA which keeps record of tracked contactees' progression separately from the rest of the infected population, which is composed of reported/hospitalized cases and unreported cases. Therefore, it has become easier to discuss the effectiveness of additional features such as isolation and monitoring protocols. The work also provides a formula for the effective reproduction number $\mathcal{R}_e$ in special cases while simulating the model under different control scenarios. Other researchers used staged-progression models to describe the impact of contact tracing on the spread of some epidemics. In (Hyman et al., 2003), authors explored the effects of random screening and contact tracing in reducing the spread of HIV. The paper (Huo, 2015) studied an age-dependent model with contact tracing. The authors provided the mathematical analysis and presented applications to smallpox and SARS(2003). Network theory has also been used to explicitly describe the contact tracing process through individual based simulation models (Keeling & Eames, 2005; Klinkenberg, Fraser, & Heesterbeek, 2006) and branching process models (Armbruster & Brandeau, 2007). This approach seems to offer better numerical simulations, yet it lacks analytical results.

On the other hand, other works were more interested in comparing the effectiveness of contact tracing in controlling infectious diseases to other containment strategies (Peak, Childs, Grad, & Buckee, 2017); Some particularly studied the influence of adopting the contact tracing intervention alongside other preventive strategies on epidemic dynamics (Almagor & Picascia, 2020; Browne, Gulbudak, & Macdonald, 2022; Choi & Shim, 2021; Quilty et al., 2021).

In this work, we develop a deterministic discrete epidemic model structured by disease-age progression that incorporates the forward dynamics of contact tracing. To this end, we link every reported case subject to screening, referred to as the "index case", with his/her transmission history made of the total effective contacts he/she has contaminated until his/her detection/isolation, then remove them from the remaining infected sub-population. We separate contact tracing intervention from other case-finding methods, including mortality reports, self-seeking health care and random testing campaigns. The separation above allows for a clear interpretation of contact tracing in relation to passive and other intervening detection actions. It also offers more flexibility in following infectees over time. Nevertheless, the two detection pathways mentioned above are complementary since contact tracing can be triggered first time by screening passively reported confirmed cases, and therefore it is important to evaluate its effectiveness in relation to other reporting actions. Taking this into consideration, the proposed model considers two main phases: initially by considering only the case-detection methods other than contact tracing, and secondly after we incorporate the first-level of contact tracing intervention, where untracked reported cases are selected as index cases and are screened for contactees. This correlates with most governments' actions during the early stages of any epidemic's emergence, by first trying classical or less costly control strategies such as social distancing and making use of available self-protective measures (Ruiz et al., 2022).

The model incorporates contact tracing in a two-step process: Firstly, we estimate the past infections caused by every index case while he/she progresses through previous disease-ages until being detected. Secondly, we explore the current status of his/her infectees, whether they are already reported or not, and determine the current disease-age of non-detected yet ones, then subtract their numbers from the remaining corresponding sub-population of infected individuals. The positivity of solutions was checked to maintain the biological meaning of the obtained results. The linearized system around the disease-free equilibrium (DFE) yields a matrix with negative entries due to the subtraction of delayed terms. Nevertheless, we applied the next-generation approach in (Cushing & Yicang, 1994) and obtained a formula for a threshold parameter $\mathcal{R}$, which is expected to be the effective reproduction number $\mathcal{R}_e$ after contact tracing incorporation. We discussed the stability of the DFE using this threshold parameter in the case where explicit calculus was possible.

To validate the proposed model, we infer the model's parameters through COVID-19 data provided by WHO for South Korea, Brazil, and Venezuela. The three countries were known to differ in contact tracing performance, where South Korea stood out as an exemplar for a better use of contact tracing in response to the pandemic during its early emergence (Emerging covid; Lewis, 2020). The obtained numerical results show the same pattern in the contact tracing efficacy of the three countries mentioned above. Thereafter, we construct an algorithm that allows a numerical estimation of the effective reproduction number $\mathcal{R}_e$ after the integration of contact tracing. The idea is based first on following the progression over time of a sample of newly infected individuals to calculate their mean survival probabilities in each age compartment while they are subject to both contact tracing and other case-detection methods. Then next, we look at the model with contact tracing as a Leslie structured model with modified progression probabilities. Furthermore, we investigate numerically the relative change of the effective reproduction number $\mathcal{R}_e$ due to contact tracing intervention related to $\mathcal{R}_0$ in the above-mentioned countries. This investigation shows, under certain assumptions, a linear dependence between the basic reproduction number $\mathcal{R}_0$ and the effective reproduction number $\mathcal{R}_e$.

2. Model framework

2.1. Base SIR discrete model with disease-age

We start with an SIR discrete compartmental model, which includes the clinical status of infected cases in the form of disease-age progression. The model also incorporates non-tracing detection/reporting of infected cases within the community. The total population size, denoted N, is divided into susceptible individuals S who are subject to contamination after exposure, infectious individuals $I = (I_k)_k$ arranged by their age of infection k, and lastly, cumulatively reported individuals R. In general, the infectious vector I is composed of latent infected cases ($I_{k\leqslant l}$) who got contaminated and pathogens had started developing within their bodies, with a mean latency period l. They become symptomatic at a mean disease-age τ, and thus by ($I_{l\leqslant k<\tau}$) we denote the compartments of pre-symptomatic cases, while ($I_{\tau\leqslant k}$) will present infected individuals with symptoms, either mild or severe, depending on the individual's duration of contamination.

We assume all infected cases $(I_k)_k$ can be detected and that any reported case in compartment R is infectiously inactive. We also cap the disease-age at a maximum of n time steps, as most cases get admitted into hospitals at some point, which usually happens when developing severe symptoms or after death. In addition, as the time scale of outbreaks is much shorter compared to the time scale of the population's growth, especially for highly contagious diseases, we neglect the demographic dynamics in the model and assume that the total population in the study remains at a constant size N over the whole epidemic outbreak duration.

For the incidence function of a vector of infected individuals $I(t) = (I_0(t)\ldots I_n(t))^T$, at a given time t, we consider the associated infectivity $\varphi(I(t))$ given by;

$$\varphi(I(t)) = \sum_{k=0}^{n} \frac{\beta_k}{N} I_k(t),$$

with $\beta_k > 0$ being the transmission rate related to the compartment I_k via the relative infectivity profile (Becker, 2015; Brauer, Feng, & Castillo-Chavez, 2010). Therefore, the transmission dynamics are then governed by a function noted $\phi(\varphi(I(t)))$, which measures the probability for susceptible individuals to survive contamination at time t after being exposed to the total infectivity $\varphi(I(t))$. The function

$$\phi : \mathbb{R}_+ \longrightarrow [0, 1],$$

known also as the "escape" function, and is a decreasing nonlinear smooth concave up function, with $\phi(0) = 1$, (Becker, 2015; Brauer et al., 2010; Diekmann, Othmer, Planqué, & Bootsma, 2021; Hernandez-Ceron, Feng, & Castillo-Chavez, 2013; Van Den Driessche & Yakubu, 2020). For example, in the case of a Poisson distributed infections (KulenoviĆ, NurkanoviĆ, & Yakubu, 2021),

$$P(m) = \frac{(\varphi(I(t)))^m}{m!} \exp(-\varphi(I(t)))$$

is the probability for a susceptible person to be infected after having m successful encounters with the total mass of infection $\varphi(I(t))$. Since the likelihood to escape infection is similar to not having any encounters with infectious cases (Allen, Jones, & Martin, 1991; Edelstein-Keshet, 2005), then

$$\phi(\varphi(I(t))) = P(0) = \exp(-\varphi(I(t))).$$

On the other hand, in the absence of contact tracing, let $\alpha_k \in [0, 1]$ be the fraction at which infectious cases from each compartment I_k are detected and reported during a single unit of time. Thus, $\alpha_k I_k$ at a given time $t \geqslant 0$ would be the number of

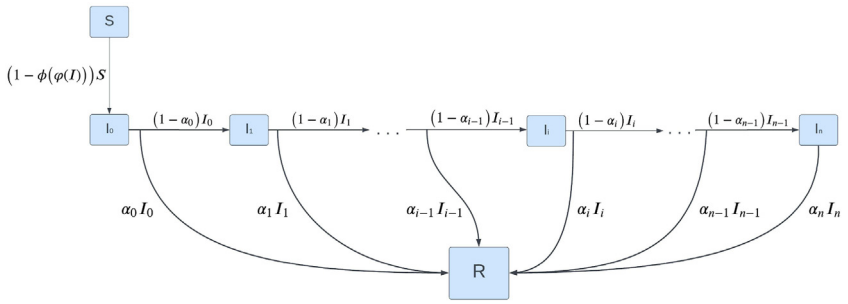

Fig. 1. Basic SIR model structured in disease-age states I_0, …, I_n.

active cases from I_k who were confirmed infected after diagnosis, got the available health care, and reported to join compartment R. Note that all infectious cases with disease-age n are always reported in the next time step, and thus α_n is assumed to be ≈ 1. Fig. 1 describes the different interactions of the basic model.

Therefore, the corresponding standard discrete staged progression system reads

$$\begin{cases} S(t+1) & = \phi(\varphi(I(t)))S(t), \\ I_0(t+1) & = (1-\phi(\varphi(I(t))))S(t), \\ I_1(t+1) & = (1-\alpha_0)I_0(t), \\ I_2(t+1) & = (1-\alpha_1)I_1(t), \\ & \vdots \\ I_n(t+1) & = (1-\alpha_{n-1})I_{n-1}(t), \\ R(t+1) & = R(t) + \sum_{k=0}^{n} \alpha_k I_k(t). \end{cases} \tag{1}$$

The model (1) is an appropriate framework for our study purposes, by providing more details in time series and allowing a smooth incorporation of contact tracing into the dynamics.

2.2. Model with contact tracing

In this section, we include the contact tracing intervention into model (1) to support and enhance the detection rate of infected active cases. As a chain process, one can distinguish between two directions of contact tracing: forward, from index cases towards their offspring contactees; and backward, from index cases towards their infectors. In practice, the direction of screening is generally unknown, however, when diseases are highly infectious, the chance of contactees being infectors is much lower than being infectees. Notably, since the infector of an index case has a greater disease-age than his/her infectees, this enhances his/her chance of being already detected when the associated index case is screened. Therefore, unless the infected population has some highly unique infective cases (super-spreaders), where backward contact tracing can be effective (Müller & Kretzschmar, 2021b; Raymenants et al., 2022), modeling forward contact tracing is more convenient. For these reasons, we will focus the present study on the forward contact tracing to be integrated into the model (1). Furthermore, we assume that contact tracing is only triggered by untracked reported active cases, with iterative tracing (screening of tracked contactees) being ignored.

According to WHO's recommended guidance, in the context of COVID-19 (World Health Organization, 2022), classical contact tracing starts by interrogating recently admitted index cases in hospitals. Tracers then prepare a list of suspected contactees, and later classify them as either confirmed after being tested positive to be immediately hospitalized, or potentially infected to be quarantined at home or in designed facilities while monitoring their status for a recommended duration. The approach we follow in this work to model contact tracing is intuitive and has been mentioned differently in some works (Browne et al., 2015; Huo, 2015). When a new case is reported, two main things should happen: investigating his/her total contribution to the infection during his/her different stages of the transmission period, and then identifying and isolating his/her infected yet undetected contactees. This can be translated in the model by shifting index cases to previous compartments with lower disease-ages, then determining their history of infection step by step from when they got infected until when they are detected/reported. Among those undetected infections, the successfully reached and diagnosed active contactees, denoted $(T_j)_{0\leqslant j\leqslant n}$, are removed from infected compartments with respect to their current age of infection.

To put that into perspective, at a given time $t \geqslant 0$, let the untracked reported cases $\alpha_k I_k(t)$ with disease-age $0 < k \leqslant n$ be our index cases. We know that their infected offspring are distributed in compartments I_j with disease-ages $0 \leqslant j < k$. Thus, theoretically, we can recalculate the contributions of these cases in the past time steps, then subtract them from compartments I_j. Note that in the model, the force of infection is governed by the non-linear function $\phi(\varphi(.))$, with input being the vector $I(.) = (I_0(.)\ldots I_n(.))^T$. Therefore, calculating the infections caused by each compartment separately back in time might not be accurate and could lead to inconsistent results. To overcome this, instead of looking for the contributions of each $\alpha_k I_k(t)$ separately, we look for the contributions of the whole vector $D(t) = (\alpha_0 I_0(t)\ldots\alpha_n I_n(t))^T \in \mathbb{R}^{n+1}$ back in time, by shifting its components, then reapplying the function $\phi(\varphi(.))$. To this end, we introduce the left-shift family of operators $(L(k))_{k\in\mathbb{N}}$ on $\mathbb{R}^{n+1}$ by

$$L(k)x = \begin{cases} (x_k, \ldots, x_n, \underbrace{0, \ldots, 0}_{\text{k elements}})^T, \text{ if } 0 \leqslant k \leqslant n, \\ (\underbrace{0, \ldots, 0}_{\text{n+1 elements}}), \text{ else}, \end{cases}$$

for all $x = (x_0, \ldots, x_n)^T \in \mathbb{R}^{n+1}$.

The vector $L(k)D(t) = (\alpha_k I_k(t), \ldots, \alpha_n I_n(t), 0, \ldots, 0)^T \in \mathbb{R}^{n+1}$ will then resume the state of D(t), k time steps prior to its detection at time t, with a change in the infectivity profiles according to k. Indeed, components of L(k)D(t) present sub-populations of the vector I(t − k)'s components with respect to disease-age at time t − k. This can also be seen by comparing the masses of infection $\varphi(L(k)D(t))$ and $\varphi(I(t-k))$ for all k ∈ {0, …, n} with t ⩾ k hereunder;

$$\begin{aligned}
\varphi(L(k)D(t)) = \sum_{j=k}^{n} \frac{\beta_{j-k}}{N} \alpha_j I_j(t) \quad &= \sum_{j=0}^{n-k} \beta_j \alpha_{j+k} I_{j+k}(t) \\
&= \sum_{j=0}^{n-k} \frac{\beta_j}{N} \alpha_{j+k} \Big(1 - \alpha_{j+k-1}\Big) I_{j+k-1}(t-1) \\
&\vdots \\
&= \sum_{j=0}^{n-k} \frac{\beta_j}{N} \left(\alpha_{j+k} \prod_{i=j}^{j+k-1} (1 - \alpha_i) \right) I_j(t-k) \\
&\leqslant \sum_{j=0}^{n} \frac{\beta_j}{N} I_j(t-k) = \varphi(I(t-k)).
\end{aligned} \tag{2}$$

The contribution of the vector L(k)D(t) in the past infections, at time t − k, is expressed as follows

$$(1 - \phi(\varphi(L(k)D(t)))) S(t-k). \tag{3}$$

However, since contacts happen randomly in the population, infection by multiple sources could take place where some infectees can be shared between L(k)D(t) and the remaining infected cases from the vector $I(t-k)$, at time t − k. To avoid recounting these common contactees between both sides, we must separate them in expression (3). For that matter, we firstly define the following family of operator $(\mathcal{C}(t,k))_{k \in \mathbb{N}}$ on $\mathbb{R}^{n+1}$ such that

$$\mathcal{C}(t,k)D(t) = I(t-k) - L(k)D(t),$$

with t ⩾ k. Each component of the vector $\mathcal{C}(t,k)D(t)$ together with its match from the vector L(k)D(t) provides the total number of infected cases within the corresponding compartment of the infectious vector I(t − k) at time t − k. Next, we decompose the expression (3) such that

$$\phi(\varphi(\mathcal{C}(t,k)D(t)))(1 - \phi(\varphi(L(k)D(t))))S(t-k) + (1 - \phi(\varphi(\mathcal{C}(t,k)D(t))))(1 - \phi(\varphi(L(k)D(t))))S(t-k). \tag{4}$$

Assuming the independence of transmission events between individuals, the second term in (4) expresses exactly the common infectees between the two groups L(k)D(t) and $\mathcal{C}(t,k)D(t)$ at time t − k. In our case, we suppose contamination intensity to be high (higher chance for effective transmission per encounter with an infectious case) and the time step to be barely enough for individuals to have many contacts (low contact rate). This ensures that newly exposed cases are not counted among the contactees of multiple index cases at once, especially during the early stages of epidemic emergence, when the population is still full of susceptible individuals with a small chance of having encounters with different infectious sources before being contaminated. Hence, with the likelihood for several infection pathways to be low, the second term in (4) can be neglected. Thus, at a given time t ⩾ 0, the cases currently with disease-age k, caused by D(t), are among those infected by L(k)D(t) at time t − k of an amount approximately given by

$$\phi(\varphi(\mathcal{C}(t,k)D(t)))(1 - \phi(\varphi(L(k)D(t))))S(t-k). \tag{5}$$

Nevertheless, the term (5) cannot be subtracted directly from the infectious sub-population with disease-age k, as a result of the contact tracing intervention at the time t. Indeed, some cases in (5) might already be confirmed and removed before tracers can reach them, either by seeking diagnosis in hospitals when feeling sick or after showing symptoms. Thus, the probability of escaping detection until the corresponding disease-age is required to be considered in the model. Note that due to the previous assumption and since iterative tracing is neglected, contactees only get tracked once their primary infector is detected. Hence, the contactees in (5) are not subject to detection by contact tracing until disease-age k. Moreover, their chance to survive non-tracing detection until the disease-age k is given by the product;

$$\left(\prod_{j=0}^{k-1}(1-\alpha_j)\right).$$

Therefore, contactees infected by L(k)D(t) at time t − k who are still infectious until the present time t are with disease-age k and are expected to be

$$\left(\prod_{j=0}^{k-1}(1-\alpha_j)\right)\phi(\varphi(\mathcal{C}(t,k)D(t)))(1-\phi(\varphi(L(k)D(t))))S(t-k). \tag{6}$$

To complete the expression (6) relative to each disease-age k ∈ {0, …, n}, we multiply by a parameter $\gamma_k \in [0,1]$ which expresses the efficacy of tracers' efforts in successfully listing, reaching, and isolating those contactees within each time step. The remaining proportion $(1-\gamma_k)$ counts then for all missed contactees or those who failed reasonable monitoring and will continue contributing in the infection until they are detected by other means, (see Fig. 2).

In the present work, we assume that the mean time delay it takes tracers to reach targeted cases and isolate them is small enough to be consumed in the time step. Indeed, some governments rely on digital tracing as an alternative option to reinforce and speed up the process (Ivers & Weitzner, 2020). Finally, at a given time t ⩾ 0, the amounts of active cases, corresponding to index cases D(t), successfully tracked and removed before reaching compartments $I_0, I_1, \ldots, I_n$ are respectively given by;

$$\begin{aligned}
T_0(t) &= \gamma_0\ \phi(\varphi(\mathcal{C}(t,0)D(t)))(1-\phi(\varphi(D(t))))S(t),\\
T_1(t) &= \gamma_1(1-\alpha_0)\ \phi(\varphi(\mathcal{C}(t,1)D(t)))(1-\phi(\varphi(L(1)D(t))))S(t-1),\\
T_2(t) &= \gamma_2(1-\alpha_0)(1-\alpha_1)\ \phi(\varphi(\mathcal{C}(t,2)D(t)))(1-\phi(\varphi(L(2)D(t))))S(t-2),\\
&\vdots\\
T_n(t) &= \gamma_n\left(\prod_{k=0}^{n-1}(1-\alpha_k)\right)\phi(\varphi(\mathcal{C}(t,n)D(t)))(1-\phi(\varphi(L(n)D(t))))S(t-n).
\end{aligned} \tag{7}$$

The formulas $T_k(t)$ in (7) provide intuitive and explicit mathematical expressions to characterise the contact tracing process. Note that (7) requires a history in time, except for the first term T_0, which represents the inhibited newly exposed cases from joining I_0, similar to an abortion effect. To this end, we introduce contact tracing to the dynamics at a time $t_0 \geq n$. Indeed, most governments prioritise other less costly containment interventions at the start of epidemics, such as confinement and social distancing (Ruiz et al., 2022), not to mention the time it takes to recruit skilled teams of tracers, especially in the case of suddenly emerged diseases.

The model (1) after implementing contact tracing becomes the system of delayed difference equations hereunder

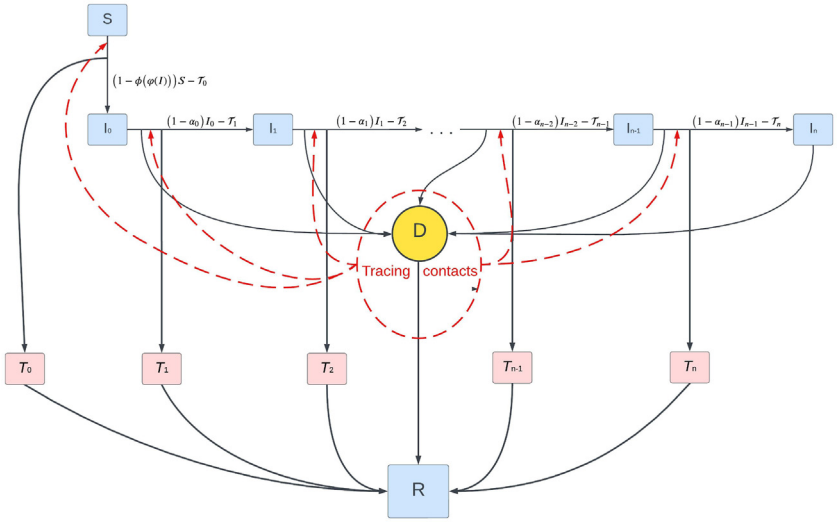

Fig. 2. The SIR model with contact tracing, triggered by untracked detected cases $D(t) = (\alpha_0 I_0(t), \ldots, \alpha_n I_n(t))^T$, in the form of $T_0(t), \ldots, T_n(t)$ removed respectively from $(1-\phi(\varphi(I(t))))S(t), (1-\alpha_0)I_0(t), \ldots, (1-\alpha_{n-1})I_{n-1}(t)$, for all t ⩾ t_0.

$$\begin{cases} S(t+1) & = \phi(\varphi(I(t)))S(t), \\ I_0(t+1) & = (1-\phi(\varphi(I(t))))S(t) - \chi_{[t_0,+\infty)}(t)T_0(t), \\ I_1(t+1) & = (1-\alpha_0)I_0(t) - \chi_{[t_0,+\infty)}(t)T_1(t), \\ I_2(t+1) & = (1-\alpha_1)I_1(t) - \chi_{[t_0,+\infty)}(t)T_2(t), \\ & \vdots \\ I_n(t+1) & = (1-\alpha_{n-1})I_{n-1}(t) - \chi_{[t_0,+\infty)}(t)T_n(t), \\ R(t+1) & = R(t) + \sum_{k=0}^{n}\Big(\alpha_k I_k(t) + \chi_{[t_0,+\infty)}(t)T_k(t)\Big). \end{cases} \tag{8}$$

where

$$\chi_{[t_0,+\infty)}(t) = \begin{cases} 1 & \text{if } t \geqslant t_0, \\ 0 & \text{if } t < t_0. \end{cases}$$

3. Positivity of solutions

The system's output measures numbers of individuals over time, which are positive quantities. Thus, for a positive initial input, the model has to provide biologically feasible solutions, which is confirmed by the next result.

Theorem 2.1. *If the initial state* $(S(0), I_0(0), \ldots, I_n(0), R(0))^T$ *of model* (8) *is in* $\mathbb{R}_+^{n+3}$, *then for all* t ∈ {1, 2, …}, *one has*

$$(S(t), I_0(t), \ldots, I_n(t), R(t))^T \in \mathbb{R}_+^{n+3}.$$

Proof. For t < t_0 the claim is obvious. When t is greater than t_0, by induction, suppose that all components of the vector $(S(s), I_0(s), \ldots, I_n(s), R(s))^T$ are positives for all $s \in \{t_0, \ldots, t\}$, and let's show that $(S(t+1), I_0(t+1), \ldots, I_n(t+1), R(t+1))^T$ remains with positive components too. From the expressions of S, I_0, R in system (8), it is clear that S(t + 1), I_0(t + 1) and R(t + 1) are positives. For k ∈ {1, …, n}, we have

$$\begin{aligned} I_k(t+1) &= (1-\alpha_{k-1})I_{k-1}(t) - T_k(t), \\ &= (1-\alpha_{k-1})[(1-\alpha_{k-2})I_{k-2}(t-1) - T_{k-1}(t-1)] - T_k(t), \\ &\vdots \\ &= \left(\prod_{i=1}^{k}(1-\alpha_{k-i})\right)I_0(t-k+1) - \sum_{j=1}^{k-1}\left(\prod_{i=1}^{k-j}(1-\alpha_{k-i})\right)T_j(t-(k-j)) - T_k(t), \\ &= \left(\prod_{i=0}^{k-1}(1-\alpha_i)\right)\left[(1-\phi(\varphi(I(t-k)))) - \sum_{j=0}^{k}\gamma_j\phi(\varphi(\mathcal{C}(t-k+j,j)D(t-k+j)))(1-\phi(\varphi(L(j)D(t-k+j))))\right]S(t-k). \end{aligned} \tag{9}$$

Thus, the proof is concluded if we show that

$$\sum_{j=0}^{k}\gamma_j\ \phi(\varphi(\mathcal{C}(t-k+j,j)D(t-k+j)))(1-\phi(\varphi(L(j)D(t-k+j)))) \leqslant (1-\phi(\varphi(I(t-k)))). \tag{10}$$

To this end, and for notation simplicity, for all j ∈ {0, …, k}, we denote

$$A_j := \varphi(L(j)D(t-k+j)).$$

Then for j ∈ {1, …, k}, one has that

$$\begin{aligned} A_j &= \sum_{i=0}^{n-j} \frac{\beta_i}{N}\ \alpha_{i+j} I_{i+j}(t-k+j), \\ &\leqslant \sum_{i=0}^{n-j} \frac{\beta_i}{N}\ \alpha_{i+j}(1-\alpha_{i+j-1}) I_{i+j-1}((t-k+j)-1), \\ &\vdots \\ &\leqslant \sum_{i=0}^{n-j} \frac{\beta_i}{N}\ \alpha_{i+j}\left(\prod_{l=i}^{i+j-1}(1-\alpha_l)\right) I_i(t-k). \end{aligned} \tag{11}$$

Hence,

$$\begin{aligned} \sum_{j=1}^{k} A_j &\leqslant \sum_{j=1}^{k-2}\sum_{i=0}^{n-j} \frac{\beta_i}{N}\ \alpha_{i+j}\left(\prod_{l=i}^{i+j-1}(1-\alpha_l)\right) I_i(t-k) \\ &+ \sum_{i=0}^{n-k+1} \frac{\beta_i}{N}\ \alpha_{i+k-1}\left(\prod_{l=i}^{i+k-2}(1-\alpha_l)\right) I_i(t-k) \\ &+ \sum_{i=0}^{n-k} \frac{\beta_i}{N}\ \alpha_{i+k}\left(\prod_{l=i}^{i+k-1}(1-\alpha_l)\right) I_i(t-k), \end{aligned} \tag{12}$$

Which means that

$$\begin{aligned} \sum_{j=1}^{k} A_j &\leqslant \sum_{j=1}^{k-2}\sum_{i=0}^{n-j} \frac{\beta_i}{N}\ \alpha_{i+j}\left(\prod_{l=i}^{i+j-1}(1-\alpha_l)\right) I_i(t-k) \\ &+ \sum_{i=0}^{n-k+1} \frac{\beta_i}{N}\ \alpha_{i+k-1}\left(\prod_{l=i}^{i+k-2}(1-\alpha_l)\right) I_i(t-k) \\ &+ \sum_{i=0}^{n-k+1} \frac{\beta_i}{N}\ (1-\alpha_{i+k-1})\left(\prod_{l=i}^{i+k-2}(1-\alpha_l)\right) I_i(t-k), \\ &\leqslant \sum_{j=1}^{k-2}\sum_{i=0}^{n-j} \frac{\beta_i}{N}\ \alpha_{i+j}\left(\prod_{l=i}^{i+j-1}(1-\alpha_l)\right) I_i(t-k) + \sum_{i=0}^{n-k+1} \frac{\beta_i}{N}\ \left(\prod_{l=i}^{i+k-2}(1-\alpha_l)\right) I_i(t-k). \end{aligned} \tag{13}$$

Iteratively, we get that

$$\sum_{j=1}^{k} A_j \leqslant \sum_{i=0}^{n} \frac{\beta_i}{N}\ (1-\alpha_i) I_i(t-k). \tag{14}$$

Therefore,

$$\begin{aligned} \sum_{j=0}^{k} A_j = A_0 + \sum_{j=1}^{k} A_j &\leqslant \sum_{i=0}^{n} \frac{\beta_i}{N}\ \alpha_i I_i(t-k) + \sum_{i=0}^{n} \frac{\beta_i}{N}\ (1-\alpha_i) I_i(t-k) \\ &\leqslant \sum_{i=0}^{n} \frac{\beta_i}{N}\ I_i(t-k) = \varphi(I(t-k)\,). \end{aligned} \tag{15}$$

Hence, for all j ∈ {0, …, k}, one can see that

$$\sum_{\substack{l=0\\ l\neq j}}^{k} A_l \leqslant \varphi(I(t-k)) - A_j = \varphi(\mathcal{C}(t-k+j,j)D(t-k+j)). \tag{16}$$

Since ϕ is a decreasing function on $\mathbb{R}_+$, then

$$\phi\left(\sum_{l\neq j}^{k} A_l\right) \geqslant \phi(\varphi(\mathcal{C}(t-k+j,j)D(t-k+j))). \tag{17}$$

Consequently,

$$\sum_{j=0}^{k} \gamma_j\, \phi(\varphi(\mathcal{C}(t-k+j,j)D(t-k+j)))(1-\phi(A_j)) \leqslant \sum_{j=0}^{k} \phi\left(\sum_{l\neq j}^{k} A_l\right)(1-\phi(A_j)). \tag{18}$$

On the other hand, using (15), we get

$$1-\phi\left(\sum_{j=0}^{k} A_j\right) \leqslant 1-\phi(\varphi(I(t-k))). \tag{19}$$

Thus, according to (18) and (19), the proof could be deducted if we show that

$$\sum_{j=0}^{k} \phi\left(\sum_{l\neq j}^{k} A_l\right)(1-\phi(A_j)) \leqslant 1-\phi\left(\sum_{j=0}^{k} A_j\right). \tag{20}$$

To do so, for m ∈ {0, …, k − 1}, let $a_m = \sum_{j=m}^{k}(1-\phi(A_j))\phi\left(\sum_{\substack{l=m\\ l\neq j}}^{k} A_l\right) + \phi\left(\sum_{j=m}^{k} A_j\right)$.

And thanks to the independence of transmission events, we get

$$a_0 = (1-\phi(A_0))\phi\left(\sum_{l=1}^{k} A_l\right) + \phi(A_0)\left[\sum_{j=1}^{k}(1-\phi(A_j))\phi\left(\sum_{\substack{l=1\\ l\neq j}}^{k} A_l\right) + \phi\left(\sum_{j=1}^{k} A_j\right)\right].$$

Thus,

$$a_0 = (1-\phi(A_0))\phi\left(\sum_{l=1}^{k} A_l\right) + \phi(A_0)a_1.$$

Similarly, one has

$$a_1 = (1-\phi(A_1))\phi\left(\sum_{l=2}^{k} A_l\right) + \phi(A_1)\left[\sum_{j=2}^{k}(1-\phi(A_j))\phi\left(\sum_{\substack{l=2\\ l\neq j}}^{k} A_l\right) + \phi\left(\sum_{j=2}^{k} A_j\right)\right].$$

Hence,

$$a_1 = (1-\phi(A_1))\phi\left(\sum_{l=2}^{k} A_l\right) + \phi(A_1)a_2.$$

Recursively, we prove that for all m ∈ {0, …, k − 2},

$$a_m = (1-\phi(A_m))\phi\left(\sum_{l=m+1}^{k} A_l\right) + \phi(A_m)a_{m+1}. \tag{21}$$

Furthermore, observe that

$$a_{k-1} = (1-\phi(A_{k-1}))\phi(A_k) + (1-\phi(A_k))\phi(A_{k-1}) + \phi(A_{k-1})\phi(A_k) \leqslant 1. \tag{22}$$

Thus, using (21) and (22), we get

$$a_{k-2} \leqslant (1-\phi(A_{k-2})) + \phi(A_{k-2}) = 1. \tag{23}$$

Iteratively, we deduce that $a_0 \leqslant 1$.

Therefore,

$$\sum_{j=0}^{k}(1-\phi(A_j))\phi\left(\sum_{l\neq j}^{k} A_l\right) \leqslant 1-\phi\left(\sum_{j=0}^{k} A_j\right), \tag{24}$$

which concludes the proof of the theorem.

4. Stability analysis

Understanding the evolution of infection reproduction over time plays a key role in predicting the dynamics of epidemics. Since contact tracing is a pre-detection tool, it affects the average transmission period of infected cases, and thus, it would be worthwhile to investigate its effect on the effective reproductive number $\mathcal{R}_e$, and eventually suggest proper actions for effective control of the pandemic.

In the case of newly emerging epidemics within a large susceptible population $S(0) \approx N$, and for t_0 small enough, we assume that $\left(\frac{I_k(t)}{N} \approx 0,\ \frac{S(t)}{N} \approx 1 \text{ for } k \in \{0,\ldots,n\} \text{ and } t \in \{0,\ldots,t_0+n\}\right)$. The linearized system of (8), around the disease free equilibrium (DFE) $\left(\tilde{S},0,\ldots,0\right)^T \in \mathbb{R}_+^{n+3}$ reads

$$\begin{pmatrix} I_0(t+1) \\ I_1(t+1) \\ \vdots \\ I_{n-1}(t+1) \\ I_n(t+1) \end{pmatrix} \approx J \begin{pmatrix} I_0(t) \\ I_1(t) \\ \vdots \\ I_{n-1}(t) \\ I_n(t) \end{pmatrix}, \quad \text{for all } t \in \{0,\ldots,t_0+n\}. \tag{25}$$

Assuming Poisson distributed infections, the Jacobian matrix J is given by

$$J = \begin{pmatrix} (1-\gamma_0\alpha_0)\beta_0 & (1-\gamma_0\alpha_1)\beta_1 & \ldots & \ldots & (1-\gamma_0\alpha_n)\beta_n \\ (1-\alpha_0) & -\gamma_1(1-\alpha_0)\alpha_1\beta_0 & \ldots & \ldots & -\gamma_1(1-\alpha_0)\alpha_n\beta_{n-1} \\ 0 & (1-\alpha_1) & \ldots & \ldots & \vdots \\ \vdots & \vdots & \vdots & & \vdots \\ 0 & 0 & \ldots & (1-\alpha_{n-1}) & -\gamma_n\left(\prod_{k=0}^{n-1}(1-\alpha_k)\right)\alpha_n\beta_0 \end{pmatrix}.$$

In the absence of contact tracing with $\gamma_0 = \ldots = \gamma_n = 0$, J becomes a Leslie matrix, and the study of the system can be found in (Allen, 2007; Brauer & Castillo-Chavez, 2014; Cushing & Yicang, 1994; Leslie, 1945) where the basic reproduction number is computed to be

$$\mathcal{R}_0 = \beta_0 + \sum_{k=1}^{n}\left(\prod_{j=0}^{k-1}(1-\alpha_j)\right)\beta_k. \tag{26}$$

After the incorporation of contact tracing, we want to have an explicit formula for the effective reproduction number $\mathcal{R}_e$. Observe that J can be presented as the sum of the two matrices

$$F = \begin{pmatrix} (1-\gamma_0\alpha_0)\beta_0 & (1-\gamma_0\alpha_1)\beta_1 & \dots & \dots & (1-\gamma_0\alpha_n)\beta_n \\ 0 & 0 & \dots & \dots & 0 \\ \vdots & \vdots & \vdots & & \vdots \\ \vdots & \vdots & 0 & & 0 \\ 0 & 0 & 0 & \dots & 0 \\ \vdots & \vdots & \vdots & & \vdots \\ 0 & 0 & \dots & 0 & 0 \end{pmatrix},$$

and

$$V = \begin{pmatrix} 0 & 0 & \dots & \dots & 0 \\ (1-\alpha_0) & -\gamma_1(1-\alpha_0)\alpha_1\beta_0 & \dots & \dots & -\gamma_1(1-\alpha_0)\alpha_n\beta_{n-1} \\ 0 & (1-\alpha_1) & \dots & \dots & \vdots \\ \vdots & \vdots & \vdots & & \vdots \\ 0 & 0 & \dots & (1-\alpha_{n-1}) & -\gamma_n\left(\prod_{k=0}^{n-1}(1-\alpha_k)\right)\alpha_n\beta_0 \end{pmatrix},$$

where F is the fertility matrix and V is the class-transitions matrix. We use the next-generation approach proposed in (Allen & Van den Driessche, 2008; Cushing & Yicang, 1994) even though it was introduced for non-negative projection matrices. So, assuming that $\rho(V) < 1$ and since only the first row in the matrix F has non-zero entries, the spectral radius $\rho\left(F(I-V)^{-1}\right)$ will be the scalar product of the first row in F and the first column in $(I - V)^{-1}$. We obtain the last by solving the system

$$(I-V)\begin{pmatrix} z_0 \\ z_1 \\ \vdots \\ z_n \end{pmatrix} = \begin{pmatrix} 1 \\ 0 \\ \vdots \\ 0 \end{pmatrix}, \text{ where } \begin{pmatrix} z_0 \\ z_1 \\ \vdots \\ z_n \end{pmatrix} \in \mathbb{R}^{n+1}. \tag{27}$$

Therefore,

$$\mathcal{R} = \rho\left(F(I-V)^{-1}\right) = (1-\gamma_0\alpha_0)\beta_0 + \sum_{k=1}^{n}((1-\gamma_0\alpha_k)\beta_k)z_k. \tag{28}$$

To check the validity of the expression (28) to be considered for the effective reproduction number, we test the stability of the DFE with respect to (28). However, for a general value of n, neither the analytical expression of (28) is easy to get nor stability analysis is obvious, due to the calculus limitation in absence of any restrictions on parameters. Thus, we consider the case when $n = 2$, for which we start by checking the feasibility of the condition $\rho(V) < 1$. Indeed, one has

$$\begin{aligned} \det(\lambda I - V) &= \begin{vmatrix} \lambda & 0 & 0 \\ -(1-\alpha_0) & \lambda + \gamma_1(1-\alpha_0)\alpha_1\beta_0 & \gamma_1(1-\alpha_0)\beta_1 \\ 0 & -(1-\alpha_1) & \lambda + \gamma_2(1-\alpha_0)(1-\alpha_1)\beta_0 \end{vmatrix}, \\ &= \lambda\left(\lambda^2 + \Gamma_0\lambda + \Gamma_1\right). \end{aligned}$$

Therefore,

$$\det(\lambda I - V) = 0 \Longleftrightarrow \lambda = 0 \text{ or } Q(\lambda) = \lambda^2 + \Gamma_0\lambda + \Gamma_1 = 0.$$

Hence,

$$\rho(V) < 1 \iff \text{ All zeros of Q lie inside the unit circle.}$$

The Jury criterion for the second degree polynomial in (Jury, 1964), then yields

$$\rho(V) < 1 \Longleftrightarrow \begin{cases} Q(1) = 1 + \Gamma_0 + \Gamma_1 > 0, \\ Q(-1) = 1 - \Gamma_0 + \Gamma_1 > 0, \\ \Gamma_1 - 1 < 0, \end{cases} \Longleftrightarrow \begin{cases} 1 - \Gamma_0 + \Gamma_1 > 0, \\ \Gamma_1 < 1. \end{cases}$$

These two conditions can be obtained for specific ranges of β_0 and β_1. For instance, a rectangle where both conditions are satisfied is given by

$$\left\{(\beta_0,\beta_1);\ \beta_0\in[0,1] \text{ and } \beta_1\in\left[0,\frac{1-(\gamma_1(1-\alpha_0)\alpha_1)(\gamma_2(1-\alpha_0)(1-\alpha_1))}{\gamma_1(1-\alpha_0)(1-\alpha_1)}\right]\right\}.$$

Next, we have the following stability result of the DFE:

Theorem 3.1. *For* $n=2$, *if* $\mathcal{R}<1$, *then DFE of* (8) *is asymptotically stable and if* $\mathcal{R}>1$, *DFE of* (8) *becomes unstable.*

Proof. When $n=2$ ($\alpha_2=1$), we have

$$\begin{cases} z_1=\dfrac{(1-\alpha_0)(1+\gamma_2(1-\alpha_0)(1-\alpha_1)\beta_0)}{(1+\gamma_1(1-\alpha_0)\alpha_1\beta_0)(1+\gamma_2(1-\alpha_0)(1-\alpha_1)\beta_0)+\gamma_1(1-\alpha_0)(1-\alpha_1)\beta_1},\\ z_2=\dfrac{(1-\alpha_0)(1-\alpha_1)}{(1+\gamma_1(1-\alpha_0)\alpha_1\beta_0)(1+\gamma_2(1-\alpha_0)(1-\alpha_1)\beta_0)+\gamma_1(1-\alpha_0)(1-\alpha_1)\beta_1}. \end{cases}$$

Let Γ_0 and Γ_1 be defined by

$$\begin{cases} \Gamma_0=\gamma_1(1-\alpha_0)\alpha_1\beta_0+\gamma_2(1-\alpha_0)(1-\alpha_1)\beta_0,\\ \Gamma_1=(\gamma_1(1-\alpha_0)\alpha_1\beta_0)(\gamma_2(1-\alpha_0)(1-\alpha_1)\beta_0)+\gamma_1(1-\alpha_0)(1-\alpha_1)\beta_1. \end{cases}$$

Therefore,

$$\mathcal{R}=(1-\gamma_0\alpha_0)\beta_0+(1-\gamma_0\alpha_1)\beta_1\frac{(1-\alpha_0)(1+\gamma_2(1-\alpha_0)(1-\alpha_1)\beta_0)}{1+\Gamma_0+\Gamma_1}+(1-\gamma_0)\beta_2\frac{(1-\alpha_0)(1-\alpha_1)}{1+\Gamma_0+\Gamma_1}.$$

On the other hand, we have

$$G(\lambda)=\det(\lambda I-J) = \begin{vmatrix} \lambda-(1-\gamma_0\alpha_0)\beta_0 & -(1-\gamma_0\alpha_1)\beta_1 & -(1-\gamma_0)\beta_2\\ -(1-\alpha_0) & \lambda+\gamma_1(1-\alpha_0)\alpha_1\beta_0 & \gamma_1(1-\alpha_0)\beta_1\\ 0 & -(1-\alpha_1) & \lambda+\gamma_2(1-\alpha_0)(1-\alpha_1)\beta_0 \end{vmatrix},$$

$$= (\lambda-(1-\gamma_0\alpha_0)\beta_0)\left(\lambda^2+\Gamma_0\lambda+\Gamma_1\right)+(1-\alpha_0)\begin{vmatrix} -(1-\gamma_0\alpha_1)\beta_1 & -(1-\gamma_0)\beta_2\\ -(1-\alpha_1) & \lambda+\gamma_2(1-\alpha_0)(1-\alpha_1)\beta_0 \end{vmatrix}.$$

Hence,

$$G(\lambda)=a_0+a_1\lambda+a_2\lambda^2+a_3\lambda^3,$$

where

$$\begin{cases} a_0= & -[((1-\gamma_0\alpha_0)\beta_0)\Gamma_1+(\gamma_2(1-\alpha_0)(1-\alpha_1)\beta_0)(1-\alpha_0)(1-\gamma_0\alpha_1)\beta_1+(1-\alpha_0)(1-\alpha_1)(1-\gamma_0)\beta_2],\\ a_1= & \Gamma_1-((1-\gamma_0\alpha_0)\beta_0)\Gamma_0-(1-\alpha_0)(1-\gamma_0\alpha_1)\beta_1,\\ a_2= & \Gamma_0-(1-\gamma_0\alpha_0)\beta_0,\\ a_3= & 1>0. \end{cases}$$

Necessary and sufficient conditions for all the zeros of F to lie inside the unit circle, are given according to Jury criteria (Jury, 1964) such that

$$G(1)>0,\quad G(-1)<0,\quad |a_0|<a_3,\ \text{ and } a_0^2-a_3^2<a_0a_2-a_1a_3. \tag{29}$$

For the first condition, we have

$$\begin{aligned} G(1) &= a_0 + a_1 + a_2 + 1 \\ &= (1 + \Gamma_0 + \Gamma_1) - (1 - \gamma_0\alpha_0)\beta_0 - ((1 - \gamma_0\alpha_0)\beta_0)\Gamma_0 - ((1 - \gamma_0\alpha_0)\beta_0)\Gamma_1 \\ &\quad -(1 - \alpha_0)(1 - \gamma_0\alpha_1)\beta_1 - (\gamma_2(1 - \alpha_0)(1 - \alpha_1)\beta_0)(1 - \alpha_0)(1 - \gamma_0\alpha_1)\beta_1 - (1 - \alpha_0)(1 - \alpha_1)(1 - \gamma_0)\beta_2 \\ &= (1 + \Gamma_0 + \Gamma_1) - (1 + \Gamma_0 + \Gamma_1)(1 - \gamma_0\alpha_0)\beta_0 - (1 + \gamma_2(1 - \alpha_0)(1 - \alpha_1)\beta_0)(1 - \alpha_0)(1 - \gamma_0\alpha_1)\beta_1 \\ &\quad -(1 - \alpha_0)(1 - \alpha_1)(1 - \gamma_0)\beta_2 \\ &= (1 + \Gamma_0 + \Gamma_1) - (1 + \Gamma_0 + \Gamma_1)\mathcal{R}. \end{aligned} \tag{30}$$

Thus,

$$G(1) = (1 + \Gamma_0 + \Gamma_1)(1 - \mathcal{R}).$$

Since $1 + \Gamma_0 + \Gamma_1 > 0$, then

$$G(1) > 0 \iff \mathcal{R} < 1. \tag{31}$$

The equivalence (31) indicates that if $\mathcal{R} > 1$, then the DFE is unstable. Indeed, since $G(1) < 0$, and $\lim_{\lambda \to +\infty} G(\lambda) = +\infty$, there exists at least $\lambda > 1$ such that $G(\lambda) = 0$.

For the rest of the proof, we assume that $\mathcal{R} < 1$ and we show that DFE is stable. In this case, the first condition in (29) holds, and we check the remaining three conditions. For the second condition, observe that

$$G(1) + G(-1) = (a_0 + a_1 + a_2 + 1) + (a_0 - a_1 + a_2 - 1) = 2(a_0 + a_2), \tag{32}$$

In addition, we have

$$\begin{aligned} \Gamma_0 &= \gamma_1(1 - \alpha_0)\alpha_1\beta_0 + \gamma_2(1 - \alpha_0)(1 - \alpha_1)\beta_0, \\ &\leqslant (\alpha_1 + (1 - \alpha_1))(1 - \alpha_0)\beta_0 = (1 - \alpha_0)\beta_0. \end{aligned} \tag{33}$$

Hence,

$$\Gamma_0 \leqslant (1 - \alpha_0)\beta_0 < (1 - \gamma_0\alpha_0)\beta_0. \tag{34}$$

Thus,

$$a_2 = \Gamma_0 - (1 - \gamma_0\alpha_0)\beta_0 < 0. \tag{35}$$

Also one can see that $a_0 < 0$, which implies that $G(1) + G(-1) < 0$. Meaning that $G(-1) < -G(1)$.

Consequently, using (31) one has $G(-1) < 0$.

For the third condition, since $a_0 < 0 < 1$, we only need to check that $-a_0 < 1$.

To this end, one has

$$G(1) = (1 + a_0) + (a_1 + a_2).$$

Moreover,

$$\begin{aligned} a_1 &= \Gamma_1 - ((1 - \gamma_0\alpha_0)\beta_0)\Gamma_0 - (1 - \alpha_0)(1 - \gamma_0\alpha_1)\beta_1, \\ &= [(\gamma_1(1 - \alpha_0)\alpha_1\beta_0)(\gamma_2(1 - \alpha_0)(1 - \alpha_1)\beta_0) - ((1 - \gamma_0\alpha_0)\beta_0)\Gamma_0] + [\gamma_1(1 - \alpha_0)(1 - \alpha_1)\beta_1 \\ &\quad -(1 - \alpha_0)(1 - \gamma_0\alpha_1)\beta_1]. \end{aligned} \tag{36}$$

Since

$$\begin{cases} 0 < \gamma_1(1 - \alpha_0)\alpha_1\beta_0 < (1 - \gamma_0\alpha_0)\beta_0, \text{ and} \\ 0 < \gamma_2(1 - \alpha_0)(1 - \alpha_1)\beta_0 < \gamma_1(1 - \alpha_0)\alpha_1\beta_0 + \gamma_2(1 - \alpha_0)(1 - \alpha_1)\beta_0 = \Gamma_0, \end{cases} \tag{37}$$

then

$$(\gamma_1(1 - \alpha_0)\alpha_1\beta_0)(\gamma_2(1 - \alpha_0)(1 - \alpha_1)\beta_0) - ((1 - \gamma_0\alpha_0)\beta_0)\Gamma_0 < 0. \tag{38}$$

Similarly, one can see that

$$\gamma_1(1-\alpha_0)(1-\alpha_1)\beta_1 < (1-\alpha_0)(1-\gamma_0\alpha_1)\beta_1. \tag{39}$$

Thus,

$$\gamma_1(1-\alpha_0)(1-\alpha_1)\beta_1 - (1-\alpha_0)(1-\gamma_0\alpha_1)\beta_1 < 0. \tag{40}$$

As a consequence, $a_1 < 0$, and by using (35), we obtain that

$$(a_1 + a_2) < 0. \tag{41}$$

Hence, $0 < G(1) < (1 + a_0)$. Therefore,

$$-a_0 < 1 \text{ and } |a_0| < 1. \tag{42}$$

For the last condition, since a_0, a_1, a_2 are all negative, then $a_0a_2 - a_1 > 0$.

Additionally, $a_0^2 - 1 = (a_0 - 1)(a_0 + 1)$. Since $(a_0 - 1) < 0$, then according to the previous implication (42) we deduce that $a_0 + 1 > 0$, and thus $a_0^2 - 1 < 0$.

Therefore,

$$a_0^2 - 1 < 0 < a_0a_2 - a_1, \tag{43}$$

which concludes the theorem.

5. Numerical results

The pandemic COVID-19 had put public health interventions under test worldwide during its early emergence. For instance, the quality of screening and tracing to mitigate outbreak waves varied depending on the available resources and the differences in terms of health-care policies.

For the numerical part of this work, we infer the model's parameters using provided data by WHO for COVID-19 for three months after the first few cases were confirmed in the considered countries, where a time step is 1 day in real life. We chose South Korea and Brazil because they are reported to have implemented contact tracing in their control protocols against the COVID-19 epidemic. We also validated the model for Venezuela as an example of a country with precarious contact tracing system (Paniz-Mondolfi, Muñoz, et al., 2020), to check whether it is capable to show the observed difference in contact tracing performance between the three countries. The choice of the countries was inspired by Oxford COVID-19 Government Response Tracker (OxCGRT) in (Which countries do covid, 2020), which gathers information on governments' interventions against the pandemic, and rank their performances through a scoring system (Hale et al., 2021).

Using the obtained parameters' values, we estimate the effective reproduction number $\mathcal{R}_e$ for the three countries, and compare their overall reproduction change while highlighting the effect of contact tracing under different control scenarios.

To begin with, the mean incubation period τ and latency period l related to COVID-19 were investigated in (Ma et al., 2020; Overton et al., 2020; Rippinger et al., 2021; Xin et al., 2022; Zhao et al., 2021). Accordingly, on average, we consider a latency of $l = 4$ days and an incubation of $\tau = 6$. The two days of difference between the two periods were due to noticeable changes in detection when transitioning from latent compartments to pre-symptomatic compartments. Indeed, data on viral transmission and the rate of false negative tests suggest that COVID-19 remains undetectable until 2 days prior to symptom onset (Jarvis & Kelley, 2021).

Next, since the maximum disease-age n is the period a newly infected case can possibly survive before death or being suspected and quarantined to neutralise its infection, it is assumed to be the sum of the mean latency period and the maximum possible infectious period. However, unlike incubation and latency which are estimated based on clinical data, the transmission period isn't easy to measure because it gets affected by control strategies and relies more on observable reports. Based on some works (Gallo et al., 2020; Hu et al., 2020; Mee et al., 2022; Vogt et al., 2022), we assume the average maximum transmission period of most infectious cases to be 12 days, and so we put $n = 16$ days. Table 1 summarises the information on the periods used.On the other hand, we consider parameters to be distributed according to the mentioned periods above, such that

$$\beta_k = \begin{cases} \tilde{\beta} & \text{if } 0 \leqslant k \leqslant l, \\ \beta & \text{if } l < k \leqslant n, \end{cases} \quad \text{and} \quad \alpha_k = \begin{cases} \alpha_0 & \text{if } 0 \leqslant k \leqslant l, \\ \alpha_1 & \text{if } l < k \leqslant \tau, \\ \alpha_2 & \text{if } \tau < k < n. \end{cases}$$

Since the early transmission of latent cases can be neglected (Liu, Magal, Seydi, & Webb, 2020), we assume $\tilde{\beta} = 0$. Also, the RT-PCR testing method has a high chance of missing latent cases, as the rate of false negative tests is high for infected cases during

Table 1
Stages of COVID-19 infection.

Time periods	Description	Mean value	References
Latent period l	time since contamination until infectiousness	4 days	(Rippinger et al., 2021; Xin et al., 2022)
Incubation period τ	time since contamination until symptoms onset	6 days	(Ma et al., 2020; Overton et al., 2020)
Transmission period n − l	time since infectiousness until isolation/ reporting	12 days	(Gallo et al., 2020; Hu et al., 2020; Mee et al., 2022; Vogt et al., 2022)

the early stages of infection (Jarvis & Kelley, 2021). Therefore, we assume that $\alpha_0 = 0$. For the contact tracing efficacies, we take $\gamma_k = \gamma$ for all $k \in \{0, \ldots, n\}$. Table 2 presents the parameters of the model to be fitted to data.

Finally, the initial state vector $(I_0(0), \ldots, I_n(0))^T$ is also fitted within a reasonable chosen range, and we assume an initial uniform distribution of infected cases at each period among the three infection stages $I_{k\leqslant l}(0)$, $I_{l\leqslant k\leqslant \tau}(0)$, $I_{k\geqslant \tau}(0)$.

5.1. Inference of parameters

We used the optimisation package curve_fit of the library scipy.optimize within the programming language Python, which utilises the classical non-linear least-squares method, to fit parameters in Table 2. Data for cumulative reported cases of COVID-19 were obtained from the official website of the World Health Organisation (WHO), as well as worldmeters, which is trusted by the American Library Association. In addition, by observing the data of daily reports and looking for massive changes in the rate of reporting, we can get an idea of when countries decided to fully incorporate contact tracing into their control plan.

We begin our estimation by fitting parameters to the cumulative reported cases data set during the first 16 days in order to acquire the initial states of infected compartments. We then fix the obtained initial state vector $(I_{k\leqslant l}(0), I_{l\leqslant k\leqslant \tau}(0), I_{k\geqslant \tau}(0))^T$ (see Table 4), and for a specific value of t_0, we refit parameters to the data set for a three-month duration (see Table 3).

The first case in South Korea was confirmed on January 20th 2020, followed by another 30 cases scattered throughout the next month, with a rate of 0–5 cases reported per day. The contact tracing was limited initially, then became comprehensive later around February 11th, to consider all detected cases as index cases (Which countries do covid, 2020). This can be noticed in Fig. 3a with a rise in daily reports four days later, where 27 cases were confirmed positive on February 15th and followed by a drastic increase in the rate of reporting on February 19th as shown in Fig. 3a. Thus, we take $t_0 = 32$.

The date January 22nd will correspond to time $t = 0$, where only one case was confirmed, thus initially $R(0) = 1$. The total population size of South Korea was around $S(0) = 51,269,185$ in 2020 (Dashboard of covidd). For the transmission rate β, the authors in (Tang et al., 2022) estimated the value of the contact rate at initial time to be 21.9 day^{-1}, and under control strategies later to be 2.01 day^{-1}, where the probability of transmission per contact was estimated to be 0.143. This corresponds respectively, to a maximum value of β of 2.89 day^{-1} and a minimum value of 0.23 day^{-1}. Therefore, we fit the transmission rate β of South Korea within the range [0, 3].

Likewise, the Brazilian health ministry notified its first case of COVID-19 on February 26th 2020, which will be taken as the starting time $t = 0$ for COVID-19 dynamics in Brazil. The country started screening confirmed cases to identify related contactees around April 1st, about a month after the first detected case (Which countries do covid; Jorge et al., 2021). This can be confirmed through Fig. 4a, when a slight increase in daily reports occurred after day 30, which continued growing for the remainder of the study period. Therefore, we choose $t_0 = 36$.The total size of the Brazilian population in 2020 was 212, 559, 417 (Dashboard of covida) which corresponds to $S(0)$ while $R(0) = 1$. According to the work (Jorge et al., 2021), we fit the transmission rate β related to Brazil within the interval [0, 2].

On the other hand, the Venezuelan government confirmed its first COVID-19 case on March 13th 2020, and a few days later put the population under total lockdown, and restricted mobility (Forero-Peña et al., 2022; Lampo et al., 2021), which limited contacts between individuals. This explained the slow epidemic growth in Venezuela compared to other countries, especially in Latin America (Burki, 2020; Lampo et al., 2021).

Table 2
Summary of fitted model parameters.

Parameters	Description	Default
$\tilde{\beta}$	transmission rate (day^{-1}) of Latent active cases.	Fixed
β	transmission rate (day^{-1}) of non-Latent active cases.	Fitted
α_0	proportion of untracked reported cases with disease-age$0\leqslant k \leqslant l$.	Fixed
α_1	proportion of untracked reported cases with disease-age$l + 1\leqslant k\leqslant \tau$.	Fitted
α_2	proportion of untracked reported cases with disease-age$\tau + 1\leqslant k \leqslant n$.	Fitted
γ	proportion of successfully tracked contactees daily of screened untracked index cases.	Fitted

Table 3
Obtained values of parameters fitted to data of cumulative reported cases of COVID-19 in S.Korea, Brazil and Venezuela since the date of first reported cases in the three countries, respectively.

Country	β	α_1	α_2	γ
S.Korea	0.87	$1.34\ 10^{-6}$	0.592	0.84
Brazil	0.77	$1.64\ 10^{-8}$	0.56	0.544
Venezuela	0.13	$2.25\ 10^{-8}$	0.01	0.11

Table 4
Fitted initial condition to first few days of cumulative reported cases with COVID-19 in the three countries before contact tracing incorporation.

Country	$I_{0\leqslant k\leqslant l}(0)$	$I_{l<k\leqslant\tau}(0)$	$I_{\tau<k\leqslant n-1}(0)$
S.Korea	1.05	0	0
Brazil	0.147	1.72	1.27
Venezuela	6.13	0	1.19

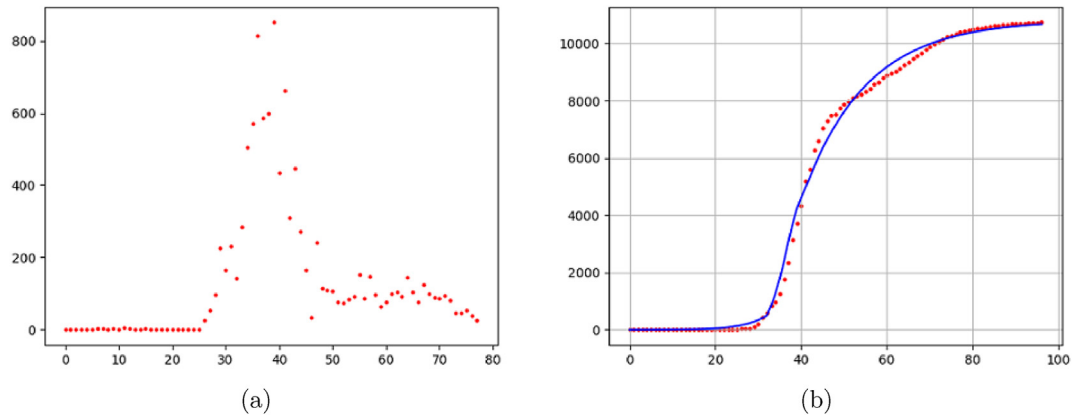

Fig. 3. (a). Data on daily reported active cases in South Korea since January 22nd to late April 2020. (b). Fitting plot of cumulative reported active cases with COVID-19 in South Korea since January 22nd to late April 2020. Data from January 22nd until February 14th is provided by WHO (Dashboard of covidc), while data from February 15th to late April 2020 is provided by Worldmeters (Dashboard of covidd).

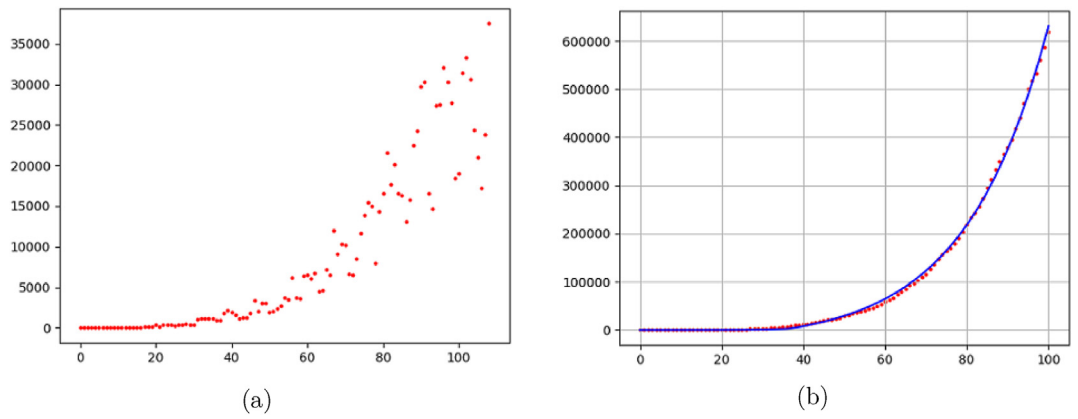

Fig. 4. (a) Data on daily active reported cases with COVID-19 in Brazil from February 26th to late May. (b) Fitting plot of cumulative reported active cases with COVID-19 in Brazil since February 26th to late May. Data is provided by Worldmeters (Dashboard of covida).

However, the transmission rate for Venezuela is fitted in [0, 2] similar to Brazil. The total size of the Venezuelan population was $S(0) = 28, 435, 940$ in 2020 (Dashboard of covide), with two confirmed cases at the initial time March 13th 2020.

According to (Which countries do covid), Venezuela didn't report using contact tracing to control COVID-19 epidemic, which possibly reflects a very low level of contact tracing practise. Up to our knowledge, no information about the date of contact tracing implementation for Venezuela is available. Nevertheless, we will evaluate our model to Venezuela's available data, and we rely mainly on the daily reports presented in Fig. 5a. Indeed, if tracing was applied even with a slight effect, it would be noticed with sudden jumps in daily reports. Thus, we take $t_0 = 38$.

Observing the values of fitted parameters in Table 3, the transmission rate in South Korea $\beta(\approx 0.8)$ correlates with the findings of (Choi & Ki, 2020) for Hubei Province. Brazil had approximately the same transmission rate. Both countries also had similar reporting distributions over disease-age $\alpha_1(\approx 0)$, $\alpha_2(\approx 0.6)$ which seems to be more focused on symptomatic cases. Venezuela, on the other hand, had a very low transmission rate $\beta(\approx 0.13)$ with negligible non-tracing detection $\alpha_1(\approx 0)$ and $\alpha_2(\approx 0.01)$. The contact tracing efficacy parameter is arranged for the above mentioned countries, such that South Korea has the highest value of $\gamma(\approx 0.8)$, followed by Brazil with an averaged value of $\gamma(\approx 0.5)$, and Venezuela has the lowest $\gamma(\approx 0.1)$.

This observed distribution of detection parameters' values mainly in South Korea and Brazil, with considerable $\gamma(\geqslant 0.5)$ and very low $\alpha_1(\approx 0)$, shows that contact tracing intervention must have greatly helped to deal with pre-symptomatic cases earlier. Indeed, Brazil likely had a massive undertesting of asymptomatic and pre-symptomatic cases during that period (Monteiro de Oliveira, Fuller, Brasil, Gabaglia, & Nielsen-Saines, 2020), while South Korea relied heavily on contact tracing to find asymptomatic cases and detect any ones with mild symptoms very early (Park et al., 2020). Most of these cases were clustered in some cities, such as Daegu and Cheonan (Shim, Tariq, Choi, Lee, & Chowell, 2020).

On the other hand, the Venezuelan parameters' obtained configuration suggest a poor detection of cases from all disease stages, which is supported by the very low testing rate in the country during that period (only 17 PCR tests per 1000 citizens) and the almost absence of any initiative testing campaigns to find asymptomatic cases (Lampo et al., 2021; Paniz-Mondolfi, Sordillo, Márquez-Colmenarez, Delgado-Noguera, & Rodriguez-Morales, 2020).

5.2. Estimation of the effective $\mathcal{R}_e$

In order to estimate $\mathcal{R}_e$ numerically, we look at the system given by model (8) as an equivalent standard Leslie's age-structured population model with modified detection probabilities due to the presence of contact tracing intervention, denoted $\tilde{\alpha_k}(t)$, of the form

$$\begin{cases} S(t+1) & = \phi(\varphi(I(t)))S(t), \\ I_0(t+1) & = (1-\tilde{\alpha_0}(t))(1-\phi(\varphi(I(t))))S(t), \\ I_1(t+1) & = (1-\tilde{\alpha_1}(t))I_0(t), \\ I_2(t+1) & = \Big(1-\tilde{\alpha}_2(t)\Big)I_1(t), \\ & \vdots \\ I_n(t+1) & = \Big(1-\tilde{\alpha}_n(t)\Big)I_{n-1}(t), \\ R(t+1) & = R(t)+\tilde{\alpha_0}(t)(1-\phi(\varphi(I(t))))S(t)+\sum_{k=1}^{n+1}\tilde{\alpha}_k(t)I_{k-1}(t). \end{cases} \tag{44}$$

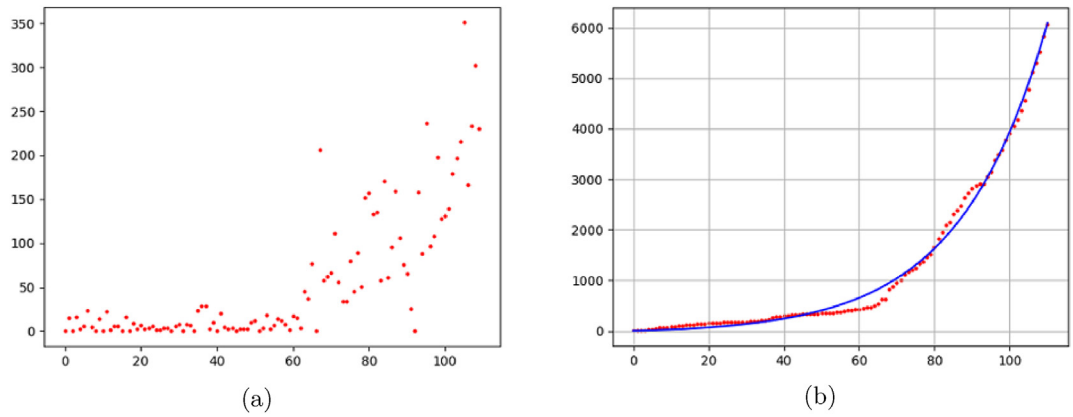

Fig. 5. (a) Data on daily reported cases in Venezuela from March 13th until mid June 2020. (b) Fitting plot of cumulative reported active cases with COVID-19 in Venezuela from March 13th until mid June 2020. Data is provided by Worldmeters (Dashboard of covide).

To calculate the modified detection probabilities for a given time $t \geqslant t_0$, we consider a starting sample group of newly infected individuals given in model (8) by $(1-\phi(\varphi(I(t))))S(t)$. Next, we follow the progression of individuals within the sample through the compartments with different disease-ages $I_0 \cdots I_n$ respectively, in times $\{t, t+1, \ldots, t+n+1\}$, and register the remaining infected cases after each time step. Then, we derive the modified survival probabilities for newly infected cases to join I_0, or cases with disease-age k to join the next compartment I_{k+1} respectively as follows

$$\begin{cases} \dfrac{I_0(t+1)}{(1-\phi(\varphi(I(t))))S(t)}, & \text{for } k=0, \\ \dfrac{I_k(t+k+1)}{I_{k-1}(t+k)}, & \text{for } k\in\{1,\ldots,n\}. \end{cases}$$

Therefore, the modified detection probabilities just before reaching the age of infection k, denoted $\tilde{\alpha}_k(t)$, are calculated by

$$\begin{cases} \tilde{\alpha}_0(t) = 1 - \dfrac{I_0(t+1)}{(1-\phi(\varphi(I(t))))S(t)}, \\ \tilde{\alpha}_k(t) = 1 - \dfrac{I_k(t+k+1)}{I_{k-1}(t+k)}, & \text{for } k\in\{1,\ldots,n\}, \\ \tilde{\alpha}_{n+1}(t) = 1. \end{cases}$$

Note that calculating these probabilities at times $\{t_0, \ldots, t_0+n\}$ might not be accurate since a perturbation in solutions occurs due to the introduction of contact tracing at time t_0, which requires a history of n steps back in time. Therefore, the modified detection probabilities will be calculated for $t \geqslant t_0 + n$. As an application, we consider Brazil's obtained configuration of parameters, and we compute these probabilities for different times $t \geqslant t_0 + n$. The resulted values, presented in Fig. 6, show that these probabilities in the presence of contact tracing are eventually constant over time. Moreover, for pre-symptomatic compartments when $k < 6$, the modified detection probabilities are enhanced remarkably due to contact tracing in the absence of detection by other means ($\alpha_0 \approx \alpha_1 \approx 0$), while for symptomatic compartments with $k \geqslant 6$ the new detection probabilities remain almost the same as the non-tracing detection probabilities ($\alpha_2 \approx 0.56$).

Furthermore, the values of $\tilde{\alpha}_k$ for the latent and pre-symptomatic classes show a decay pattern, apart from the first probabilities $\tilde{\alpha}_0$, $\tilde{\alpha}_1$, $\tilde{\alpha}_2$, which are organised differently. Nevertheless, the effect of contact tracing is clearly observed in the compartments with low disease-ages, supporting the claim that contact tracing handled pre-symptomatic cases more efficiently than symptomatic ones in Brazil.

Since we assumed that the time for contact tracing implementation was not large, the population of susceptible individuals remains relatively almost the same, and the population of infected individuals is still negligible compared to the total population size N. Thus, similar to the formula of the net reproduction number in (Batista, 2021; Cushing & Yicang, 1994; Tuljapurkar & Caswell, 2012), the effective reproduction number is given by

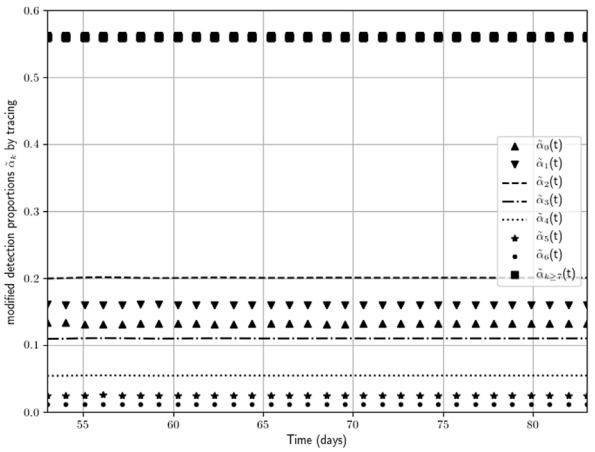

Fig. 6. The modified detection proportions after contact tracing implementation at time $t_0 = 36$, for Brazil's fitted parameters; $\beta = 0.77$, $\alpha_1 \approx 0$, $\alpha_2 = 0.56$ and $\gamma = 0.54$, calculated for different samples taken at times $t \geqslant t_0 + 16 = 52$. The proportions $\tilde{\alpha}_k(t)$ with $k \in \{7, \ldots 17\}$ are all presented with square-dashed line and have approximately the same value of ≈ 0.56.

$$\mathcal{R}_e = \sum_{k=0}^{n} \left(\prod_{j=0}^{k} (1 - \tilde{\alpha}_j) \right) \beta_k, \tag{45}$$

where $\left(\prod_{j=0}^{k}(1-\tilde{\alpha}_j)\right)$ is the probability to survive detection by all means, when contact tracing is initiated, since infection until disease-age k.

To support the legitimacy of the expression, we test the stability of the DFE with respect to the threshold $\mathcal{R}_e$. In the absence of contact tracing, the epidemic dynamics are observed through the basic reproduction number $\mathcal{R}_0$. So we consider the Brazil's initial state $(S(0), I_{0\leqslant k\leqslant l}(0), I_{l<k\leqslant\tau}(0), I_{\tau<k\leqslant n}(0), R(0))^T$ mentioned above, with $\beta = 0.77$ and $\alpha_2 = 0.8$. We then vary α_1 to obtain values of $\mathcal{R}_0$ close enough to unity above and below, as shown in Fig. 7a. When $\mathcal{R}_0 < 1$, the infection dies out over time, whereas if $\mathcal{R}_0 > 1$, it persists and continues growing slowly until it eventually reaches the epidemic peak.

For the case when incorporating contact tracing, we use the Brazil's obtained configuration of detection parameters, where $\alpha_1 \approx 0$ and $\alpha_2 = 0.56$, in order to get a higher value of $\mathcal{R}_0 (\approx 2.91)$. After including the contact tracing into the system at time t_0, the epidemic dynamics can now be observed through the threshold $\mathcal{R}_e$, as seen in Fig. 7b. If $\mathcal{R}_e < 1$, the infection starts decaying slowly over time, while in case $\mathcal{R}_e > 1$, it continues on growing.

5.3. Comparison of contact tracing performance

To get a better overview of the impact of contact tracing on epidemic dynamics in the three countries, we start by checking the expected time since infection until detection and isolation before and after its implementation at time t_0 in the system. For that matter, we build up the probability distribution for infected cases to be reported after spending a certain period post-exposure, as can be seen in Table 5.where

$$\begin{cases} \delta_k = \prod_{j=0}^{k-1} \left(1 - \tilde{\alpha}_j\right) \tilde{\alpha}_k, \text{ for } k \in \{1 \ldots n+1\}, \\ \delta_0 = \tilde{\alpha}_0. \end{cases}$$

Table 6 shows the obtained values for the mean disease-age $\mathbb{E} = \left(\sum_{k=1}^{n+2} k\ \delta_{k-1} \right) - 1$ when a case is reported. It represents the case of a sample infected at a time $t < t_0$ before tracing implementation and the case of a sample infected at a time $t \geqslant t_0 + n$ after the contact tracing intervention had taken place.

The values presented in Table 6, clearly show how efficient contact tracing was in suppressing the lifespan of infected individuals for the three countries, and the extent of its performance in controlling the disease spread;

In South Korea, the mean value of the disease-age when cases are reported was reduced from 7.69 days down to 2.36 days, which represents almost half latency period l (=4 days) of COVID-19 disease. Meaning that most newly infected cases are reported about 2 days after exposure on average, showing the successful response to interrupt transmission chains after index

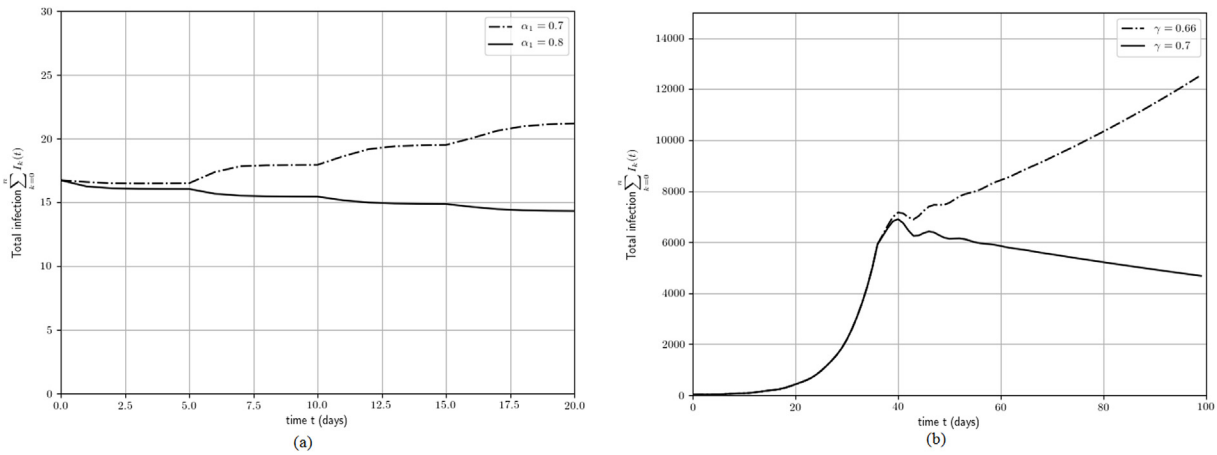

Fig. 7. (a). Plot of the total infection $\|I(.)\|_1$ over time, in the absence of contact tracing. The dashed line represents the case when $\mathcal{R}_0 = 1.08$ and the solid line represents the case when $\mathcal{R}_0 = 0.96$. (b). Plot of the total infection $\|I(.)\|_1$ over time, when incorporating contact tracing at time $t_0 = 36$ for different values of γ. For $t < t_0$, $\mathcal{R}_0 = 2.91$. For $t \geqslant t_0$, the dashed line represents the case where $\mathcal{R}_e = 1.06$, and the solid line is for $\mathcal{R}_e = 0.96$.

Table 5
Probability distribution δ_k to be reported after infection by a period of k days.

Time since infection until detection and isolation	0 days	1 day	2 days	…	16 days	17 days
Probability to be reported	δ_0	δ_1	δ_2	…	δ_n	δ_{n+1}

Table 6
Mean disease-ages when infected cases are reported, before and after contact tracing incorporation, for the three countries.

Country	$\mathbb{E}$ (before tracing)	$\mathbb{E}$ (after tracing)
S.Korea	7.69	2.36
Brazil	7.78	4.34
Venezuela	16.46	15.37

case screening. This is also supported by the observational study in (Park et al., 2020), showing that most of the 7812 admitted patients during the first 3 months of COVID-19 emergence in South Korea, were either asymptomatic or had mild illness.

Similarly, in Brazil, we observe that most infected cases were reported past 4 days on average. This was obviously highly effective, especially with the high transmission rate $\beta(\approx 0.77)$ and the undertesting of pre-symptomatic cases in the country (Monteiro de Oliveira et al., 2020; Neiva et al., 2020). Whereas, in the case of Venezuela, contact tracing, if used, didn't have much effect on the mean period after which infected cases are reported (≈ 16). It was still too high, leaving enough room for outbreaks to occur.

Furthermore, by using the acquired values of fitted parameters in Table 3, and expression (26) we estimated the basic reproduction number $\mathcal{R}_0$ for South Korea to be 3.21, where the authors in (Kim et al., 2020; Tang et al., 2022) suggested $\mathcal{R}_0$ to be 1.77 and 2.6 respectively. For Brazil, we obtained $\mathcal{R}_0 = 2.91$, while it was estimated in the works (de Souza et al., 2020; Kumari, Kumar, Sharma, Singh, & Parshad, 2023) to be 3.1. Finally, in Venezuela, we obtained $\mathcal{R}_0 = 1.68$, while authors in (González-Parra, Díaz-Rodríguez, & Arenas, 2022) found $\mathcal{R}_0 = 1.9$. One can see that the estimated values of $\mathcal{R}_0$ for the three countries seem to correlate with the suggested approximations presented by the different works mentioned above.

After the contact tracing incorporation in the three countries, we use formula (45) to estimate the effective $\mathcal{R}_e$, where the obtained values are presented in Table 7. For South Korea, we estimated the effective reproductive number $\mathcal{R}_e$ to be 0.64, noting that the authors in (Choi & Ki, 2020) had found the initial reproduction number around February 19th to be $\mathcal{R}(0) = 0.5$, which corresponds to the time after the comprehensive contact tracing is considered. In Brazil, we found $\mathcal{R}_e$ to be 1.38, which correlates with the findings in (Almeida, Vilches, Ferreira, & Fortaleza, 2021), where the authors showed that the average value of the epidemic reproduction coefficient kept fluctuating between 1. and 2.5 for the following 4 months after April 1st. For Venezuela, we obtained $\mathcal{R}_e = 1.48$.

To assess the effectiveness of contact tracing, we calculate the relative variation of the reproduction number due to its implementation as a preventive measure

$$\Delta r = \frac{\mathcal{R}_0 - \mathcal{R}_e}{\mathcal{R}_0},$$

where the calculated values are presented in Table 7. We observe that in South Korea, the government achieved up to 80 % reduction in the reproductive number from 3.21 to 0.64. On the other hand, in Brazil, the reproductive number was reduced noticeably by 52 %, lowering its value from initially 2.91 down to 1.38. Lastly, for Venezuela, the reproductive number was decreased from 1.68 to 1.48 resulting in a reduction of 11 %.

Looking at the obtained values in Table 7, one can see that contact tracing had the most effect on controlling the COVID-19 outbreak in South Korea among the three countries during the study period. Brazil also benefited considerably from the intervention, but not as much as South Korea, which might have been related to the difference in testing rates between the two countries at that time (Neiva et al., 2020). Contact tracing in Venezuela, if used, had very weak influence on epidemic dynamics, which is most likely linked to the very low testing interventions in the country during the study period (Lampo et al., 2021).

On the other hand, one can see that the values of Δr for each of the three countries are approximately equal to the associated contact tracing efficacy parameter γ. This has inspired us to plot the factor $\frac{\mathcal{R}_e}{\mathcal{R}_0}$ against the parameter γ, which resulted in approximate lines, as can be seen in Fig. 8. This allows us to consider the following linear dependence between $\mathcal{R}_e$ and $\mathcal{R}_0$ as follows

Table 7
The reproduction number, before and after contact tracing strategy incorporation, and its relative change for the three countries, compared to contact tracing efficacy γ.

Country	$\mathcal{R}_0$	$\mathcal{R}_e$	Δr	γ
S.Korea	3.21	0.64	0.8	0.84
Brazil	2.91	1.38	0.525	0.544
Venezuela	1.68	1.48	0.11	0.11

$$\mathcal{R}_e \approx (1 - A\gamma)\mathcal{R}_0. \tag{46}$$

According to expression (46), the effect of contact tracing on epidemic transmission is resumed by the term Aγ, where $A = A(\beta, \alpha_2)$. We can further explore how the coefficient $A \approx 1 - \frac{\mathcal{R}_e}{\mathcal{R}_0}|_{\gamma=1}$ changes when varying the two parameters α_2 and β as can be seen in Fig. 9. We observe in this scenario that A doesn't change much when varying the transmission rate β. Additionally, A increases drastically when increasing α_2, with an almost saturation effect when the values of α_2 are high enough.Moreover, it is clear in Fig. 9a that for high values of α_2, the coefficient A becomes much closer to 1. Therefore expression (46) becomes

$$\mathcal{R}_e \approx (1 - \gamma)\mathcal{R}_0. \tag{47}$$

We continue our analysis to reach a simplified expression for $\mathcal{R}_e$, thus we take α_2 within a reasonable range such that $A \approx 1$. In real life, when tracers list contactees of screened index cases, they are uncertain which of them are already reported, and which of them are still active in the population. Therefore, the efficacy of contact tracing γ stands for the proportion of listed and removed contactees with success, regardless of whether they are removed by tracers or not. In addition, since in this work all index cases are untracked reported cases, the average number they infected throughout their infectious period is $\mathcal{R}_0$.

Let p be the proportion of infectees that were detected, but not by tracing, among the offspring of an index case. Thus, $\gamma(1-p)\mathcal{R}_0$ is the amount of infectees removed by tracers, per index case. On the other hand, $\gamma p\mathcal{R}_0$ are tracked infectees who were already removed by other detection ways when reached by tracers. Therefore, the average number of secondary infected contactees successfully listed and isolated per primary reported index case is given by the sum $\gamma(1-p)\mathcal{R}_0 + \gamma p\mathcal{R}_0$, which is $\gamma\mathcal{R}_0$. Note that the isolation of cases here simply means they are no longer able to spread infection.

As a consequence, expression (46) can be reformulated such that

$$\mathcal{R}_e \approx (\gamma\mathcal{R}_0)\frac{(1-\gamma)}{\gamma}. \tag{48}$$

In (Browne et al., 2015), the authors proved a similar formula to $\mathcal{R}_e$ under the following assumptions: Firstly, perfect reporting, where all cases are eventually reported and no unreported cases exist. Secondly, perfect monitoring, which means that the transmission of tracked reported cases is neglected. Thirdly, most contactees are tracked while still incubating. The first two assumptions are clearly taken into consideration by our model. The last can be seen through the modified probabilities presented earlier in Fig. 6, where the effect of contact tracing was negligible post-incubation.

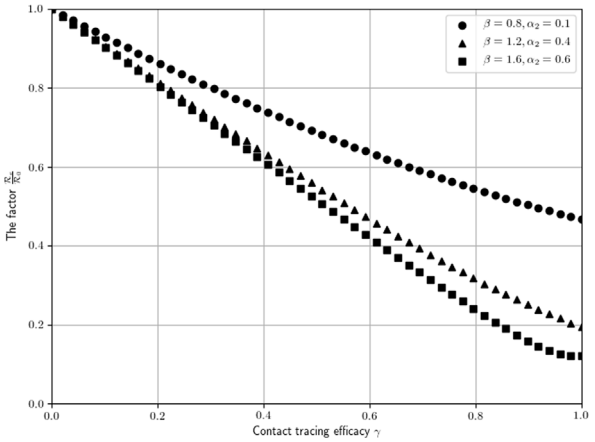

Fig. 8. (a). Plot of the factor $\frac{\mathcal{R}_e}{\mathcal{R}_0}$ against contact tracing efficacy γ for different values of parameters β and α_2 with $\alpha_1 \approx 0$. The circle line in case $\beta = 0.8$, $\alpha_2 = 0.1$, the triangle line in the case $\beta = 1.2$, $\alpha_2 = 0.4$ and the square line in the case $\beta = 1.6$, $\alpha_2 = 0.6$.

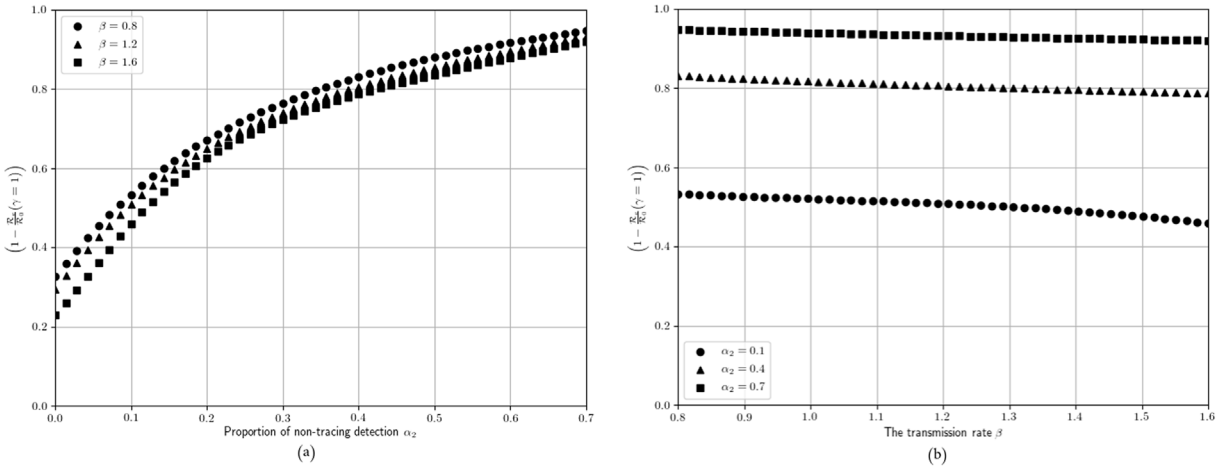

Fig. 9. (a). Plots of the coefficient A against α_2 for different values of β with $\alpha_1 \approx 0$. (b). Plots of the coefficient A against β for different values of α_2 with $\alpha_1 \approx 0$.

6. Conclusions and discussion

This study aimed to provide a simple yet informative model to analyze the impact of contact tracing alongside the other case-detection methods of infected individuals on the growth of transmissible diseases within communities. We proposed a discrete model with disease-age progression over two main phases: before the incorporation of contact tracing, with other case-detection ways to mitigate infection, and after its incorporation, with both detection options coupled to influence the system's outcomes.

For positive input, the model provided positive solutions over time with no restrictions on parameters. We tested the next-generation approach to the system, although the projection matrix governing the linearized system about the DFE has some negative entries related to the subtraction of the delayed terms generated by contact tracing. This yielded an explicit formula for a threshold parameter $\mathcal{R}$, expected to be the effective reproduction number $\mathcal{R}_e$, yet still required a rigorous proof to confirm. Nevertheless, the formula was partially backed up with stability analysis of the DFE only when n = 2, because of calculus limitations, and left the general case for an upcoming work.

We fitted the model's parameters to data on the COVID-19 pandemic in some countries during a period of three months after the first case was reported in each of them. We selected South Korea and Brazil mainly as two countries known to implement contact tracing interventions in their control strategies against COVID-19 and also included Venezuela, which declared almost no screening reports, as can be seen in Fig. 3b, 4b and 5b. Moreover, the obtained values of fitted parameters for South Korea and Brazil also confirm the observed pattern in contact tracing performances.

The formula of $\mathcal{R}_e$ was deduced numerically using an algorithm based on substituting model (8) with an alternative equivalent version that includes contact tracing into new modified detection probabilities per disease-age given by model (44). We then evaluated the relative change in the reproduction number Δr, using the obtained fitted parameters' values as given in Table 7. We found that its values were approximately similar to those of the contact tracing efficacy γ, which suggested a linear dependence between $\mathcal{R}_0$ and $\mathcal{R}_e$. This was confirmed by plotting the factor $\frac{\mathcal{R}_e}{\mathcal{R}_0}$ against γ as shown in Fig. 8, yielding the approximation $\mathcal{R}_e \approx (1 - A\gamma)\mathcal{R}_0$. We also found that the coefficient A depends mainly on non-tracing detection. This leads us to believe that the coefficient A might describe the fraction of untracked reported cases among the total reported cases of each generation. Thus, $A\mathcal{R}_0$ would be the offspring of the untracked reported index cases. The obtained approximation then makes sense, as $\mathcal{R}_e$ after incorporating contact tracing is the total offspring $\mathcal{R}_0$ of infectious cases excluding the tracked infectees $\gamma A\mathcal{R}_0$.

This formulation of $\mathcal{R}_e$ shows that the effect of contact tracing on the epidemic dynamics is unaffected by the fatality of the disease, but rather depends on the performance of both detection pathways, as can be seen in Fig. 9. So increasing the impact of contact tracing requires either increasing the detection of index cases or increasing the number of tracked infectees per index case. Increasing the non-tracing detection of cases would probably mean investing more in random mass testing of the population. On the other hand, successfully tracking more infectees per index case requires, for example, expanding the size of the tracer workforce. Both investments are costly, however putting too much effort in increasing the non-tracing detection is not worth it past a certain threshold. It is confirmed with the almost saturation effect shown in Fig. 9. Nevertheless, this raises the need for an optimal control study to determine the best way to manage the resources.

The model overall offered acceptable results, which encourages including and testing additional features of contact tracing, especially with that form of discrete model that isn't abundantly used in literature. In fact, we intend on including a flexible time period m < n, where only infectees with a disease-age lower than m are eligible to be tracked. Indeed, we suspect the effect of contact tracing starts fading in classes with older disease-ages, which was seen earlier in Fig. 6. In addition, we

also plan on adding the size of the tracer workforce to the model and studying its relation to m with the purpose of finding an optimal strategy for efficient contact tracing.

Funding

The authors would like to thank the Infectious Disease Modelling Journal for the total waiver of the publication fees on the occasion of the no article processing charge open access week from October 23 to 29, 2023.

Declaration of interest statement

We wish to confirm that there are no known conflicts of interest associated with this publication titled "Mathematical modeling of contact tracing and stability analysis to inform its impact on disease outbreaks; an application to COVID-19", and there has been no specific financial support for this work that could have influenced its outcome.

CRediT authorship contribution statement

Mohamed Ladib: Writing – original draft, Methodology, Investigation. **Aziz Ouhinou:** Supervision, Methodology, Investigation. **Abdul-Aziz Yakubu:** Formal analysis.

Declaration of generative AI and AI-assisted technologies in the writing process

During the preparation of this work, the authors used the "free Scribbr online service" in order to check and correct language errors in the manuscript. After using this "free Scribbr online service," the authors reviewed and edited the content as needed and take full responsibility for the content of the publication.

References

Allen, L. (2007). *An introduction to mathematical biology*. Pearson/Prentice Hall.
Allen, L., Jones, M., & Martin, C. (1991). A discrete-time model with vaccination for a measles epidemic. *Mathematical Biosciences, 105*(1), 111–131.
Allen, L., & Van den Driessche, P. (2008). The basic reproduction number in some discrete-time epidemic models. *Journal of Difference Equations and Applications, 14*(10–11), 1127–1147.
Almagor, J., & Picascia, S. (2020). Exploring the effectiveness of a covid-19 contact tracing app using an agent-based model. *Scientific Reports, 10*, Article 22235.
Almeida, G., Vilches, T., Ferreira, C., & Fortaleza, C. (2021). Addressing the covid-19 transmission in inner Brazil by a mathematical model. *Scientific Reports, 11*, Article 10760.
Armbruster, B., & Brandeau, M. (2007). Contact tracing to control infectious disease: When enough is enough. *Health Care Management Science, 10*(4), 341–355.
Batista, M. (2021). On the reproduction number in epidemics. *Journal of Biological Dynamics, 15*(1), 623–634.
Becker, N. (2015). *Modeling to inform infectious disease control*. CRC Press.
Brauer, F., & Castillo-Chavez, C. (2014). *Mathematical models in population biology and epidemiology*. Springer.
Brauer, F., Feng, Z., & Castillo-Chavez, C. (2010). Discrete epidemic models. *Mathematical Biosciences and Engineering, 7*(1), 1–15.
Browne, C., Gulbudak, H., & Macdonald, J. (2022). Differential impacts of contact tracing and lockdowns on outbreak size in covid-19 model applied to China. *Journal of Theoretical Biology, 532*, Article 110919.
Browne, C., Gulbudak, H., & Webb, G. (2015). Modeling contact tracing in outbreaks with application to ebola. *Journal of Theoretical Biology, 384*, 33–49.
Burki, T. (2020). Covid-19 in Latin america. *The Lancet Infectious Diseases, 20*(5), 547–548.
Choi, S., & Ki, M. (2020). Estimating the reproductive number and the outbreak size of covid-19 in korea. *Epidemiology and Health, 42*, Article e2020011.
Choi, W., & Shim, E. (2021). Optimal strategies for social distancing and testing to control covid-19. *Journal of Theoretical Biology, 512*, Article 110568.
Cushing, J., & Yicang, Z. (1994). The net reproductive value and stability in matrix population models. *Natural Resource Modeling, 8*(4), 297–333.
Dashboard of covid-19 cases for brazil. https://www.worldometers.info/coronavirus/country/brazil/. Accessed since 2020-01-03.
Dashboard of covid-19 cases for countries of the world. https://www.worldometers.info/coronavirus/.
Dashboard of covid-19 cases for south korea by who. https://covid19.who.int/region/wpro/country/kr. Accessed since 2020-01-03.
Dashboard of covid-19 cases for south korea by worldmeters. https://www.worldometers.info/coronavirus/country/south-korea/. Accessed since 2020-01-03.
Dashboard of covid-19 cases for venezuela. https://www.worldometers.info/coronavirus/country/venezuela/. Accessed since 2020-01-03.
de Souza, W., Buss, F., Candido, D., Carrera, J., Li, S., Zarebski, A., et al. (2020). Epidemiological and clinical characteristics of the early phase of the covid-19 epidemic in Brazil. *Nature Human Behaviour, 4*, 856–865.
Diekmann, O., Othmer, H., Planqué, R., & Bootsma, M. (2021). The discrete-time kermack–mckendrick model: A versatile and computationally attractive framework for modeling epidemics. *Proceedings of the National Academy of Sciences, 118*(39), Article e2106332118.
Edelstein-Keshet, L. (2005). *Mathematical models in biology*. SIAM.
Emerging covid-19 success story: South korea learned the lessons of mers. https://ourworldindata.org/covid-exemplar-south-korea. Accessed since 2021-03-05.
World Health Organization. (2022). *Contact tracing and quarantine in the context of covid-19: Interim guidance, 6 july 2022*. World Health Organization.
Forero-Peña, D., Carrión-Nessi, F., Mendoza-Millán, D., Omaña-Ávila, Ó., Mejía-Bernard, M., Camejo-Ávila, N., et al. (2022). First wave of covid-19 in Venezuela: Epidemiological, clinical, and paraclinical characteristics of first cases. *Journal of Medical Virology, 94*(3), 1175–1185.
Gallo, L., Oliveira, A., Abrahao, A., Sandoval, L., Martins, Y., Almirón, M., et al. (2020). Ten epidemiological parameters of covid-19: Use of rapid literature review to inform predictive models during the pandemic. *Frontiers in Public Health, 8*, Article 598547.
González-Parra, G., Díaz-Rodríguez, M., & Arenas, A. (2022). Mathematical modeling to study the impact of immigration on the dynamics of the covid-19 pandemic: A case study for Venezuela. *Spatial and Spatio-temporal Epidemiology, 43*, Article 100532.
Hale, T., Angrist, N., Goldszmidt, R., Kira, B., Petherick, A., Phillips, T., et al. (2021). A global panel database of pandemic policies (oxford covid-19 government response tracker). *Nature Human Behaviour, 5*(4), 529–538.

Hernandez-Ceron, N., Feng, Z., & Castillo-Chavez, C. (2013). Discrete epidemic models with arbitrary stage distributions and applications to disease control. *Bulletin of Mathematical Biology, 75*(10), 1716–1746.
Hossain, A., Jarolimova, J., Elnaiem, A., Huang, C., Richterman, A., & Ivers, L. (2022). Effectiveness of contact tracing in the control of infectious diseases: A systematic review. *The Lancet Public Health, 7*(3), e259–e273.
Hu, Z., Song, C., Xu, C., Jin, G., Chen, Y., Xu, X., et al. (2020). Clinical characteristics of 24 asymptomatic infections with covid-19 screened among close contacts in nanjing, China. *Science China Life Sciences, 63*(5), 706–711.
Huo, X. (2015). Modeling of contact tracing in epidemic populations structured by disease age. *Discrete and Continuous Dynamical Systems - Series B, 20*(6), 1685–1713.
Hyman, J., Li, J., & Stanley, E. (2003). Modeling the impact of random screening and contact tracing in reducing the spread of hiv. *Mathematical Biosciences, 181*(1), 17–54.
Ivers, L., & Weitzner, D. (2020). Can digital contact tracing make up for lost time? *The Lancet Public Health, 5*(8), e417–e418.
Jarvis, K., & Kelley, J. (2021). Temporal dynamics of viral load and false negative rate influence the levels of testing necessary to combat covid-19 spread. *Scientific Reports, 11*, 9221.
Jorge, D., Rodrigues, M., Silva, M., Cardim, L., da Silva, N., Silveira, I., et al. (2021). Assessing the nationwide impact of covid-19 mitigation policies on the transmission rate of sars-cov-2 in Brazil. *Epidemics, 35*, Article 100465.
Jury, E. (1964). *Theory and application of the z-transform method*. Wiley.
Keeling, M., & Eames, K. (2005). Networks and epidemic models. *Journal of the Royal Society Interface, 2*(4), 295–307.
Kim, S., Jeong, Y., Byun, J., Cho, G., Park, A., Jung, J., et al. (2020). Evaluation of covid-19 epidemic outbreak caused by temporal contact-increase in South Korea. *International Journal of Infectious Diseases, 96*, 454–457.
Klinkenberg, D., Fraser, C., & Heesterbeek, H. (2006). The effectiveness of contact tracing in emerging epidemics. *PLoS One, 1*(1), e12.
KulenoviĆ, M., NurkanoviĆ, M., & Yakubu, A. (2021). Asymptotic behavior of a discrete-time density-dependent si epidemic model with constant recruitment. *Journal of Applied Mathematics and Computing, 67*, 733–753.
Kumari, N., Kumar, S., Sharma, S., Singh, F., & Parshad, R. (2023). Basic reproduction number estimation and forecasting of covid-19: A case study of India, Brazil and Peru. *Communications on Pure and Applied Analysis, 67*(2), 417–440.
Kwok, K., Tang, A., Wei, V., Park, W., Yeoh, E., & Riley, S. (2019). Epidemic models of contact tracing: Systematic review of transmission studies of severe acute respiratory syndrome and middle east respiratory syndrome. *Computational and Structural Biotechnology Journal, 17*, 186–194.
Lampo, M., Hernández-Villena, J., Cascante, J., Vincenti-González, M., Forero-Peña, D., Segovia, M., et al. (2021). Signatures of the venezuelan humanitarian crisis in the first wave of covid-19: Fuel shortages and border migration. *Vaccines, 9*(7), 719.
Leslie, P. (1945). On the use of matrices in certain population mathematics. *Biometrika, 33*(3), 183–212.
Lewis, D. (2020). Where covid contact-tracing went wrong. *Nature, 588*, 384–387.
Liu, Z., Magal, P., Seydi, O., & Webb, G. (2020). A covid-19 epidemic model with latency period. *Infectious Disease Modelling, 5*, 323–337.
Ma, S., Zhang, J., Zeng, M., Yun, Q., Guo, W., Zheng, Y., et al. (2020). Epidemiological parameters of covid-19: Case series study. *Journal of Medical Internet Research, 22*(10), Article e19994.
Mee, P., Alexander, N., Mayaud, P., Gonzalez, F., Abbott, S., de Souza Santos, A., et al. (2022). Tracking the emergence of disparities in the subnational spread of covid-19 in Brazil using an online application for real-time data visualisation: A longitudinal analysis. *The Lancet Regional Health-Americas, 5*, Article 100119.
Monteiro de Oliveira, M., Fuller, T., Brasil, P., Gabaglia, C., & Nielsen-Saines, K. (2020). Controlling the covid-19 pandemic in Brazil: A challenge of continental proportions. *Nature Medicine, 26*, 1505–1506.
Müller, J., & Kretzschmar, M. (2021a). Contact tracing–old models and new challenges. *Infectious Disease Modelling, 6*, 222–231.
Müller, J., & Kretzschmar, M. (2021b). Forward thinking on backward tracing. *Nature Physics, 17*, 555–556.
Neiva, M., Carvalho, I., Costa Filho, E., Barbosa-Junior, F., Bernardi, F., Sanches, T., et al. (2020). Brazil: The emerging epicenter of covid-19 pandemic. *Revista da Sociedade Brasileira de Medicina Tropical, 53*, Article e20200550.
Overton, C., Stage, H., Ahmad, S., Curran-Sebastian, J., Dark, P., Das, R., et al. (2020). Using statistics and mathematical modelling to understand infectious disease outbreaks: Covid-19 as an example. *Infectious Disease Modelling, 5*, 409–441.
Paniz-Mondolfi, A., Muñoz, M., Florez, C., Gomez, S., Rico, A., Pardo, L., et al. (2020). Sars-cov-2 spread across the colombian-venezuelan border. *Infection, Genetics and Evolution, 86*, Article 104616.
Paniz-Mondolfi, A., Sordillo, E., Márquez-Colmenarez, M., Delgado-Noguera, L., & Rodriguez-Morales, A. (2020). The arrival of sars-cov-2 in Venezuela. *Lancet (London, England), 395*(10236). e85–e86.
Park, H., Lee, J., Lim, N., Lim, D., Hong, S., Park, M., et al. (2020). Presenting characteristics and clinical outcome of patients with covid-19 in South Korea: A nationwide retrospective observational study. *The Lancet Regional Health-Western Pacific, 5*, Article 100061.
Peak, C., Childs, L., Grad, Y., & Buckee, C. (2017). Comparing nonpharmaceutical interventions for containing emerging epidemics. *Proceedings of the National Academy of Sciences, 114*(15), 4023–4028.
Perra, N. (2021). Non-pharmaceutical interventions during the covid-19 pandemic: A review. *Physics Reports, 913*, 1–52.
Quilty, B., Clifford, S., Hellewell, J., Russell, T., Kucharski, A., Flasche, S., et al. (2021). Quarantine and testing strategies in contact tracing for sars-cov-2: A modelling study. *The Lancet Public Health, 6*(3), e175–e183.
Raymenants, J., Geenen, C., Thibaut, J., Nelissen, K., Gorissen, S., & Andre, E. (2022). Empirical evidence on the efficiency of backward contact tracing in covid-19. *Nature Communications, 13*, 4750.
Rippinger, C., Bicher, M., Urach, C., Brunmeir, D., Weibrecht, N., Zauner, G., et al. (2021). Evaluation of undetected cases during the covid-19 epidemic in Austria. *BMC Infectious Diseases, 21*, 70.
Ruiz, Y., Vecino-Ortiz, A., Guzman-Tordecilla, N., Peñaloza-Quintero, R., Fernández-Niño, J., Rojas-Botero, M., et al. (2022). Cost-effectiveness of the covid-19 test, trace and isolate program in Colombia. *The Lancet Regional Health-Americas, 6*, Article 100109.
Rusu, A., Emonet, R., & Farrahi, K. (2021). Modelling digital and manual contact tracing for covid-19. are low uptakes and missed contacts deal-breakers? *PLoS One, 16*(11), Article e0259969.
Schneiders, M., Naemiratch, B., Cheah, P., Cuman, G., Poomchaichote, T., Ruangkajorn, S., et al. (2022). The impact of covid-19 non-pharmaceutical interventions on the lived experiences of people living in Thailand, Malaysia, Italy and the United Kingdom: A cross-country qualitative study. *PLoS One, 17*(1), Article e0262421.
Shim, E., Tariq, A., Choi, W., Lee, Y., & Chowell, G. (2020). Transmission potential and severity of covid-19 in South Korea. *International Journal of Infectious Diseases, 93*, 339–344.
Tang, B., Xia, F., Bragazzi, N., McCarthy, Z., Wang, X., He, S., et al. (2022). Lessons drawn from China and South Korea for managing covid-19 epidemic: Insights from a comparative modeling study. *ISA Transactions, 124*, 164–175.
Tsimring, L., & Huerta, R. (2003). Modeling of contact tracing in social networks. *Physica A: Statistical Mechanics and Its Applications, 325*(1–2), 33–39.
Tuljapurkar, S., & Caswell, H. (2012). *Structured-population models in marine, terrestrial, and freshwater systems*. Springer.
Van Den Driessche, P., & Yakubu, A. (2020). Age structured discrete-time disease models with demographic population cycles. *Journal of Biological Dynamics, 14*(1), 308–331.
Vogt, F., Kurup, K., Mussleman, P., Habrun, C., Crowe, M., Woodward, A., et al. (2022). Contact tracing indicators for covid-19: Rapid scoping review and conceptual framework. *PLoS One, 17*(2), Article e0264433.
Which countries do covid-19 contact tracing? https://ourworldindata.org/grapher/covid-contact-tracing. Oxford COVID-19 Government Response Tracker, Blavatnik School of Government, University of Oxford. Accessed since 2020-01-01.

Xin, H., Li, Y., Wu, P., Li, Z., Lau, E., Qin, Y., et al. (2022). Estimating the latent period of coronavirus disease 2019 (covid-19). *Clinical Infectious Diseases, 74*(9), 1678–1681.
Zhao, S., Tang, B., Musa, S., Ma, S., Zhang, J., Zeng, M., et al. (2021). Estimating the generation interval and inferring the latent period of covid-19 from the contact tracing data. *Epidemics, 36*, Article 100482.